AD_____

Award Number: DAMD17-03-1-0193

TITLE: Biological Effects of Activating Distinct ErbB Receptor Dimers in Polarized Growth Arrested Epithelia

PRINCIPAL INVESTIGATOR: Marissa Nolan

CONTRACTING ORGANIZATION: Cold Spring Harbor Laboratory
Cold Spring Harbor, NY 11724

REPORT DATE: September 2006

TYPE OF REPORT: Annual Summary

PREPARED FOR: U.S. Army Medical Research and Materiel Command
Fort Detrick, Maryland 21702-5012

REPORT DOCUMENTATION PAGE

Form Approved
OMB No. 0704-0188

1. REPORT DATE	2. REPORT TYPE	3. DATES COVERED
01-09-2006	Annual Summary	16 Aug 2003 – 15 Aug 2006

4. TITLE AND SUBTITLE

Biological Effects of Activating Distinct ErbB Receptor Dimers in Polarized Growth Arrested Epithelia

5a. CONTRACT NUMBER

5b. GRANT NUMBER
DAMD17-03-1-0193

5c. PROGRAM ELEMENT NUMBER

6. AUTHOR(S)

Marissa Nolan

5d. PROJECT NUMBER

5e. TASK NUMBER

5f. WORK UNIT NUMBER

7. PERFORMING ORGANIZATION NAME(S) AND ADDRESS(ES)

Cold Spring Harbor Laboratory
Cold Spring Harbor, NY 11724

8. PERFORMING ORGANIZATION REPORT NUMBER

9. SPONSORING / MONITORING AGENCY NAME(S) AND ADDRESS(ES)
U.S. Army Medical Research and Materiel Command
Fort Detrick, Maryland 21702-5012

10. SPONSOR/MONITOR'S ACRONYM(S)

11. SPONSOR/MONITOR'S REPORT NUMBER(S)

12. DISTRIBUTION / AVAILABILITY STATEMENT
Approved for Public Release; Distribution Unlimited

13. SUPPLEMENTARY NOTES
Original contains colored plates: ALL DTIC reproductions will be in black and white.

14. ABSTRACT

ErbB family of receptor tyrosine kinases have been implicated in human breast cancers. In particular ErbB2 is over expressed in 25-35% of all breast cancers. We can selectively activate a particular receptor using a chimeric system and synthetic ligand. We combine this system with a three-dimensional cell culture system, which allow cells to grow into mammary acini like structures in vitro. We have shown that activation of ErbB2 induces a change in cell polarity and re-initiates proliferation in 3D structures. Using these systems we have investigated how activation of ErbB2 disrupts epithelial cell polarity and disrupts proliferation control. In particular, we studied how the Par complex and Rho family of small GTPases regulate ErbB2-induced transformation of human mammary epithelial cells. We have shown that activated ErbB2 recruits Par6 and disrupts the par complex. We have also shown that interfering with the functional complex by expressing a Par6 mutant prevents ErbB2 from fully transforming mammary epithelial cells. In our efforts to understand the effect of deregulating the function of Par protein complex, we made the unexpected observation that overexpression of Par6 induced growth-factor independent proliferation of mammary epithelial cells. Understanding how these proteins affect proliferation and cell polarity and their relationship to Erbb2 will identify diagnostic markers and drug targets to treat breast cancer.

15. SUBJECT TERMS
ErbB, Polarity, Proliferation, Mammary Epithelial cell biology, Three Dimensional, Par complex

16. SECURITY CLASSIFICATION OF:				18. NUMBER OF PAGES	19a. NAME OF RESPONSIBLE PERSON
					USAMRMC
a. REPORT	b. ABSTRACT	c. THIS PAGE			19b. TELEPHONE NUMBER *(include area code)*
U	U	U	UU	59	

Standard Form 298 (Rev. 8-98)
Prescribed by ANSI Std. Z39.18

Table of Contents

Introduction: Malignant breast cancer develops from transformed mammary epithelial cells. These transformed cells form early lesions that are characterized by loss of epithelial architecture and uncontrolled proliferation. Currently early lesions are defined using histological techniques but the molecular features that distinguish different histological types are not known. Correlating these molecular alterations with histopathology could serve to predict the outcome of early stage lesions and design better treatments. Although oncogenes implicated in breast cancer have been described, how they specifically interfere with tissue architecture giving rise to different histopathological patterns remain to be elucidated.

ErbB receptor network and breast cancer: ErbB receptors are a family of receptor tyrosine kinases (RTKs) that are important during normal development and tumorigenesis of the mammary gland. Many biological processes are regulated by ErbB receptors such as cell division, migration, adhesion, differentiation, morphogenesis and prevention of apoptosis[1]. There are four members in this family, ErbB1 (EGFR, HER1), ErbB2 (HER2/Neu), ErbB3 and ErbB4. Over-expression of ErbB family members is associated with breast, ovary, brain and prostate cancers. ErbB2 is over-expressed in 25-30% of breast cancers. ErbB2 gene amplification and overexpression also correlates with a poor clinical prognosis[2, 3].

Epithelial cell polarity: Mammary epithelial cells line the ducts of the mammary gland and possess an apical-basal polarity as defined by their ability to localize their cell-cell junctions (tight junctions, gap junctions, and adherens junctions) and their proteins asymmetrically along the apical-basal axis. Establishment of apical-basal cell polarity requires the concerted efforts of a series of protein complexes that create and maintain the spatial asymmetry. Recent studies have identified three protein complexes the Par complex (Par3, Par6, aPKC, Cdc42/Rac), the Scribble complex (Scribble, Lgl, Dlg), and the Crumbs complex (Crumbs, Pals, PATJ) that act in a cooperative manner to establish apical-basal polarity [4-6]. Members of these complexes are thought to cross-talk with each other. However, the results of this cross-talk and their individual functions remain unclear. In addition to being part of the Par complex, Par6 also interacts with the crumbs complex and the Scribble complex suggesting that Par6 may play and important role in coordinating the interaction with other polarity complexes [7]. Recent evidence suggests that alterations in the polarity machinery may contribute to oncogenesis. Loss of LKB1 (Par4) and Dlg5 are predisposition factors for human cancer [8] and the human papillomavirus protein E6, targets scribble for degradation[9]. It has also been shown that Par6 cooperates with RacV12 to transform fibroblasts[10]. In addition, overexpression of aPKC has been shown in NSCL and ovarian carcinoma. Increase expression of aPKC promoted aberrant proliferation and loss of cell polarity in ovarian epithelia [11-13]. Although it is not known how this machinery interplays with extracellular signaling cues to adapt cell architecture these studies are outlining the role of polarity regulators in oncogenic signaling.

Rho GTPase family and cancer: Rho family members are known to play important roles in regulating epithelial cell polarity for instance, Rac and CDC42 are part of the Par protein complex and play critical roles during establishment of epithelial cell polarity. Rho proteins can cycle between GTP and GDP bound states, which are effected by a variety of different regulator molecules that either promote or inhibit GTP binding. They are categorized into three different subgroups based on similarity to RhoA, Rac1 and Cdc42, and proteins that lack GTPase activity. Rho GTPases are over-expressed in human breast, colon, lung and pancreatic cancers [14]. Specifically RhoA, Rac1 and Cdc42 are over-expressed in breast cancer [15]. Since then, there have been no reports mutated Rho proteins in tumors. The

evidence suggests that it is cycling of GDP/GTP that is important for transformation [16, 17]. Other studies show that Rac activity is increased in breast cancer cell lines[14, 18]. The accumulating evidence suggests that it is the deregulation of these proteins that correlates with tumor progression and poor prognosis[14].

Specific synthetic ligand mediated ErbB dimerization: ErbB receptors have the ability to homo and heterodimerize generating complex signaling networks. Our lab has circumvented this problem by using a chimeric ErbB receptor. The chimera can bind to synthetic ligand, dimerize, phosphorylate, and generate downstream signals. This system allows us to specifically activate the receptor of interest [19].

Cell culture system: Our lab combines this a unique system to study the inducible effects of ErbB receptors with a three-dimensional cell culture system. In the past it has been difficult to study the relationship between oncogenes and architecture due to a lack of tractable in vitro models. We have also set up a culture system for human mammary epithelial cells (MCF-10A) on a matrix abundant in collagen and laminin (Matrigel). In this environment, cells can grow from a single cell to into 3D acini-like structures with a single layer of epithelial cells surrounding a luminal space. These 3D acini structures have characteristics similar to the resting epithelium of mammary glands, such as low proliferation rate and organized architecture. MCF-10A cell lines have been established that express ErbB1 (B1) and ErbB2 (B2) chimeras using a retroviral expression system. We have shown that activation of ErbB2 cells in the 3D system induces multilayering, changes in cell polarity and re-initiates proliferation [20]. This resembles the early stages of transformation in vivo and thus is an excellent model to study the important factors in the initiation of the oncogenic process. However, activation of ErbB1 does not induce transformation of resting structures, suggesting that ErbB2 has specific signaling pathways to transform organized epithelial cells possibly by modulating epithelial cell architecture.

<u>Body</u>:

In this annual summary we show:

Activation of ErbB2 disrupts epithelial cell polarity prior to initiating cell proliferation.
Activation of ErbB2 disrupts the Par complex and associates with Par6.
Mutant Par6 overexpression prevents ErbB2 induced multi-structures.
Par6 overexpression induces EGF independent proliferation in 2D and 3D cell culture.
Par6 overexpression sustains MAPK cell proliferation signaling.

Task 1. To determine if different ErbB dimers differ in their ability to induce proliferation in growth arrested epithelia and in their ability to affect cell polarity in polarized growth arrested epithelia.

Chemical inhibition of ErbB2 induced proliferation: We have previously established an ErbB activation assay in Madin-Darby Canine Kidney epithelial cells (MDCK)[20]. Upon activation of ErbB2 in a polarized growth arrested monolayer proliferation is reinitiated (BrdU incorporation), apical-basal polarity is disrupted (ZO-1 mislocalization) and cells begin to multilayer. Activation of ErbB1 showed no changes in proliferation or polarity in polarized growth arrested epithelial. From this point on I concentrated on the elucidation of ErbB2's mechanism while utilizing ErbB1 activation as a control. Using this activation assay we wanted to separate ErbB2's ability to reinitiate proliferation from polarity disruption. I proposed utilization of commercially available chemical inhibitors to interfere with proliferation pathways. I then activated ErbB2 in the presence of MAPK and Src Kinase inhibitors (Figure1). I observed that both proliferation and apical basal polarity disruption were dependent on Src Kinase activity while inhibition of MAPK did not block polarity disruption. I conclude that ErbB2, not ErbB1 stimulation reinitiates proliferation in polarized growth arrested epithelial in a MAPK and Src

Kinase dependent manner. Additional experiments will be done to verify that Src Kinase is necessary for apical-basal polarity disruption.

Task 2. Determine if there is a hierarchal relationship between the signal to disrupt polarity and the signal to reinitiate proliferation

I have previously observed ErbB2 induced disruption of polarity within six hours of activation, followed by reinitiation of proliferation 15 hours post activation. This observation of polarity disruption as a primary effect and proliferation as a secondary effect was followed in collaboration with other members of our laboratory. The effect of ErbB2 activation on apical-basal polarity, proliferation and multilayering were monitored in an extensive time course of activation. The mislocalization of ZO-1 down the lateral membrane was quantitated through high-resolution microscopy. The normal localization of ZO-1 was restricted to 2 μm from the apical surface, detection of ZO-1 below 2 μm was considered mislocalized. Reinitiation of proliferation was monitored by flow cytometry and multilayered epithelial cells were quantitated by measuring the area where 2 or more cells overlap in different focal plans (Appendix IV/Figure 1). We quantitatively determined that ErbB2 first targeted the tight junctions prior to reinitiation of proliferation and subsequent multilayering. This conclusion allowed us to focus our studies on how ErbB2 disrupts cell polarity.

Task 3. Define the mechanism by which ErbB2 disrupts cell polarity and forms multi-acinar structures.

A. Characterization of RhoGTPase activation/inhibition in ErbB2 induced transformation of polarized epithelia. The Rho family of GTPases have been shown to be downstream of ErbB2. Activation of ErbB2 re-initiates proliferation and induces disruption of 3D acini structures forming multi-acinar structures. I investigated whether interfering with the Rho family inhibits the ErbB2 induced phenotype. In order to pursue this task I decided to generate and establish a working adenoviral system with the ability to infect polarized growth arrested epithelial cells. I also decided to generate reagents to constitutively express target proteins to validate the adenoviral expression system.

Generation of Adenoviral vector expressing Cdc42N17, RhoN19 and RhoAWT: Since, I am interested in inducing expression of genes in proliferation-arrested cells, I decided to adapt an inducible adenoviral expression system to carry out these studies. I utilized a vector backbone (obtained from J. Chernoff) and generated adenoviral expression vectors that allow for tetracycline regulated protein and IRES GFP expression. I successfully generated a Cdc42N17, RhoN19 and RhoWT adenoviral vectors from expression plasmids, pCG CDC42N17 pCDNA RhoAWT and pGBT8 RhoN19 (obtained from Linda Van Alest's). Adenovirus was successfully generated with Cdc42N17 and RhoN19. I also obtained existing adenovirus RacV12, RacN17, RhoV14, RhoN19, Cdc42L61 and control GFP from J.Chernoff. I utilized both dominant negative and activated RhoGTPase viruses for immediate experimentation.

Determination of optimal adenoviral infection conditions and cell line: I had a choice of two different cell lines MDCK and mammary epithelial (MCF-10A). Although MDCK cells are well suited for generation of polarized monolayers, I was unable to obtain high infection efficiency in polarized growth arrested monolayers. However, MCF-10A cells were easily infected with adenovirus and had robust protein expression with viral titers of 300 –30 particles/cell (Figure 2 and 3). I decided to use MCF-10A cells for subsequent experiments for 4 reasons: (1) they are derived from human breast tissue making them relevant to breast cancer, (2) they have the ability to generate acini structures in 3D which

recapitulate the organization of epithelial in vivo better then monolayer culture, (3) they can be infected easily and (4) our lab is well experienced in using MCF-10A cells as a tool. Therefore I used this model system to study the effects of deregulation of Rho GTPase signaling in both forming and developed 3D structures.

Expression of Rho family proteins during formation of mammary acini: For these experiments MCF-10A cells were plated in 3D growth conditions. The cells were infected on Day 2 (d2) and the acini were allowed to develop for 4 – 10 days. Both RhoN19 and RacN17 had an effect on the developing acini structures (Figure 4A). The cells lost their ability to form organized acini structures, allowing for protrusions and blebbing formation. Expression of activating mutations of the RhoGTPases also prevented the proper development of acini structures (Data not shown). This data suggests that proper RhoGTPases regulation is required for the establishment of 3D epithelial architecture.

Expression of Rho family proteins in fully formed mammary acini: For these experiments MCF-10A cells were plated on 3D growth conditions. The cells developed into acini structures for 8 days and were then infected (d8) and allowed to express protein for 4 days. Neither RacN17 nor RhoN19 appeared to perturb the organized acinar structures as the infected acini were indistinguishable from control (Figure 4B). Together these data suggests that Rho and Rac are important for development but not in maintenance of the acini structure. All activating RhoGTPase mutations and Cdc42N17 expressed in developed acini structures perturbed the organization of the acini (data not shown). Therefore I only considered Rho and Rac dominant negative proteins expressed in conjunction with ErbB2 activation for further analysis. The data is summarized in Table 1.

Activation of ErbB2 in conjunction with RhoN19 and RacN17 expression in Day 12 structures: Expression of RacN17 had no effect on ErbB2 induced phenotype. Interestingly, there seems to be a cooperative effect between RhoN19 expression and ErbB2 activation (Figure 5A and B). The structures show changes in morphology, and their architecture is disrupted with protrusions and blebbing (Figure 5B). The blebbing morphology is quantitated in figure 6 showing that only upon ErbB2 stimulation does RhoN19 promote disruption. Apart from these morphological differences, ErbB2 is still able to re-initiate proliferation in the presence of RhoN19 expression as determined by Ki-67 proliferation marker (data not shown) and formation of multistructures is not affected. Since RhoN19 expression does not affect proliferation or multistructure formation I decided to focus on acinar morphology. Normal acini secrete a polarized layer of extracellular matrix (ECM) composed of collagen and laminin. I observed in RhoN19 expressing ErbB2 activated structures the ECM that surrounds the acini is altered. The cooperative effect of RhoN19 and ErbB2 activation disrupts organized laminin (Figure 7A and B). Since breakdown of ECM is one characteristic of invasive cells I utilized an invasion assay where the acini are embedded in a mixture of collagen and matrigel. Our preliminary experiments (data not shown) suggest that these blebbing protrusions have the ability to invade the surrounding matrix. I plan to do RNAi experiments of RhoA and RhoC to verify this cooperative phenotype and study the downstream pathways. Interestingly, a recent study has shown that RNAi of RhoA, not RhoC, promoted invasion in two different breast cancer cell lines supporting the idea that Rho downregulation plays a role in promoting invasion [21].

B. Introduction of polarity complex mutations to interfere with ErbB2 induced transformation of polarized growth arrested epithelia.

The above results suggest a role for polarity regulators in modulating oncogenic signaling. We wanted to test this by investigating the role of Par6 an important polarity regulator. Previous results from our lab suggested that the par complex may also be a target for ErbB2 therefore we designed experiments to test this using mutational analysis of the scaffolding components of Par6

Generation of Par6 mutations in retroviral vectors: The functional Par complex is composed of Par3, Par6, aPKC, and cdc42/Rac. Par6 has also been shown to bind other polarity proteins such as Crumbs and Lgl. Mutations in Par6 have been generated that interfere with its ability to bind effector molecules. To date the C-terminal Flag tagged Par6 full length, N-terminal Flag tagged Par6 Full length, Par6 C-Term aa140-345, PDZ domain, and point mutations $Par6^{\Delta pro136}$ (Δcdc42), $Par6^{K19A}$ (Δapkc), $Par6^{M235W}$ (ΔLgl/Pals1) are in retroviral vectors (Figure 8).

ErbB2 inducibly binds Par6: In collaboration with lab members we determined that Par6 binds to activated ErbB2 receptor in an immunoprecipitation assay. Both endogenous and overexpressed flag-par6 are capable of forming a physical complex with activated ErbB2. This is demonstrated in appendix IV/Figure 2. Appendix IV/Figure 2 also shows that activation of ErbB2 disrupts the association of Par3 and aPKC. Together this data suggests that activation of ErbB2 regulates the Par polarity complex and subsequently disrupts epithelial cell polarity.

Par6K19A overexpression inhibits ErbB2 induced multi-aciniar structures: In order to investigate the role of Par6 in ErbB2 induced multistructure formation we expressed a mutant version of Par6. When ErbB2 is activated in the presence of wild type Par6 we see multi-structure formation. However, upon activation in the presence of $Par6^{K19A}$ (Δapkc), ErbB2 is defective in promoting multi-acinar formation. Interestingly, $Par6^{K19A}$ is capable of binding to ErbB2 (Appendix IV/Figure 3) and ErbB2 is still able to reinitiate proliferation when $Par6^{K19A}$ (Appendix IV/Figure 4). This data suggests that ErbB2 needs to recruit a functional Par complex to disrupt 3D epithelial acini. Therefore separating ErbB2's ability to promote proliferation from it's ability to disrupt epithelial cell architecture.

C. Characterization of Par6 and mutations in control MCF-10A cells

Full-length Par6 expression induced EGF independent growth on 2D: Under normal cell culture conditions MCF-10A cells require EGF to grow. Cells will significantly slow their growth in EGF depleted media. I have previously observed that full-length par6 expressing cell line proliferated rapidly in EGF free media when compared to control cells infected with empty vector, and parental MCF-10A cells (Figure 9A and B). I verified this observation in another EGF dependent cell line, CommaD (Figure 10A and B). This is an exciting observation, as growth factor independence is a hallmark for transformation so I proceeded to characterize how Par6 can play a role in promoting proliferation.

Verification of Par6 over-expression phenotype: I have observed a consistent two-fold increase in S-phase (Flow Cytometry analysis of propidium iodide stain) with par6 expression (Figure 11). All original observations were made with overexpression of C-terminal Flag tagged Full length Par6α in MSCV PURO IRES GFP. I wanted to control for the location of the epitope tag and expression levels. To do this I generated cell lines expressing variable levels of C-terminal Flag Par6 and N-terminal Flag Par6. I observed a 2-fold increase in S-phase of Par6 expressing cells regardless of expression level or location of the epitope tag. I also wanted to determine if the different isoforms of Par6 confer EGF independence. When I overexpressed Par6β I saw the same phenotype as Par6α (Figure 11) . Since I was able to verify the EGF independent phenotype in the 2D system I am interested in determining the effects of Par6 when applied to a polarized context as in our 3D model system.

Par6 overexpression sensitizes cells to EGF in 3D matrigel assay: Previously I have shown that Par6 overexpression affects the normal development of the acini structures in the presence of EGF. The structures grow larger in Par6 expressing cells, I assayed acini size using phase contrast imaging and zeiss software to generate the area of an acini (Figure 12A) I have also shown that, when EGF is removed after 4 days of development only the Par6 cells continue to grow larger once EGF is removed (Figure 12A). This led us to propose that Par6 is sensitizing the cells to EGF induced proliferation. In order to decipher cell size from proliferation, I decided to use lower concentration of EGF than what is required for normal acinar development. I monitored acini size (Figure 12B) and also counted cell

nuclei/acini using DAPI stain (Figure 13A). I determined that Par6 cells are sensitized to proliferation when grown in low amounts of EGF as monitored by Ki67 (proliferation marker) immunoflourescence in Figure 13B. Thus, I have determined that the increase in Par6 acini size is due to proliferation. Immunofluoresence of Par6 acini structures determined that lumens have been cleared through apoptosis and that cell polarity, as defined by golgi marker and laminin, remains normal (data not shown). In order to rule out cell line specific effects I verified the EGF sensitization in a mouse mammary epithelial cell line (HC11) that also forms 3D structures. I was able to observe par6 cooperation with EGF to promote acini morphogenesis in HC11 cells (Figure 14). Since I have determined and verified that Par6 overexpression increases proliferation in 2D and 3D systems I want to determine the effectors that Par6 is utilizing to confer this EGF independent proliferation. In order to address this I have taken a biochemical and structure function approaches.

Par6 requires a functional complex to promote EGF independent proliferation: Structure function analysis will allow us to determine what Par6 effector proteins are responsible for EGF independent proliferation. Data suggests that C-Terminal truncation and Par6 PDZ do not confer EGF independent proliferation. Expression of Par6 point mutations Δpro136, K19A and M235W all interfere with the ability of Par6 to promote EGF independent proliferation (figure 15A and B). Expression of Par6K19A in the 3D assay did not promote 3D morphogenesis when compared to wild type Par6 (Figure 16). A summary of constructs and subsequent phenotypes are depicted in Table 2. When I interfere with known Par6 effector binding, I inhibit the ability of Par6 to generate EGF independent proliferation. This implies the ability of Par6 to promote EGF independent proliferation is related to its known effector interactions.

Verification of effector binding: Immunopreciptiations were performed using anti-flag antibodies. I have shown that K19A does not bind aPKC, and that Δpro136 does not bind cdc42. Currently, I have no antibody to detect Lgl or Pals binding to the M235W and this is in process of being addressed (Figure 17).

Inhibition of aPKC in Par6 overexpressing cell lines: Since all of the mutations generated interfere with aPKC function I would like to verify that its activity is required for EGF independent growth. To do this I will take two approaches to determine if aPKC is responsible for the proliferation: a chemical inhibitor of aPKC and a dominant negative version of aPKC. One possibility is that inhibition of aPKC reduces the ability of Par6 to promote EGF independent proliferation. Other possibilities would be no effect or increase in proliferation. However, since aPKC is a major binding partner of Par6 I expect its inhibition to interfere with the function of Par6.

Biochemical:

Chemical inhibition of proliferation pathways prevents Par6 induced EGF independent proliferation: I wanted to determine which pathways Par6 is using to promote proliferation. It was observed that inhibition of MAPK pathway (U0126), PI3K (LY294002), and Src Kinase (PP2) inhibited EGF independent proliferation (Figure 18A). I further characterized the phenotype using inhibitors of EGFR (AG-1478), ErbB2 (AG-825), and MTOR (Rapamycin) pathways. Only inhibition of EGFR abolishes the proliferation phenotype (Figure 18B). I will verify this by using different methods of EGFR inhibition such as antibody inhibitors (IMC-C255). Since inhibition of EGFR interfered with proliferation I want to determine whether Par6 interferes/potentates EGFR signaling.

Par6 over-expression sustains Erk1/2 phosphorylation: Activation of EGFR and RTKs results in activation Ras/MAPK pathway and an increase in ERK1/2 phosphorylation leading to cell proliferation. I have determined that activation of Erk1/2 is sustained compared to mscv control cells and $Par6^{K19A}$ (figure 19). In order to determine the specificity of this activation, I looked at other known signaling pathways. In particular the PI3K pathway, phosphorylation of AKT was not increased in Par6

overexpressing cells compared to MSCV control. This data suggests that Par6 is cooperating with EGF/EGFR pathway to induce cell proliferation.

Protein Expressed	Successful Generation	Phenotypic observation in D12 3D structures	Activation of ErbB2 phenotype in structures
Cdc42N17	Yes	Disruption of architecture	Disruption of architecture
*RacN17	Yes	None observed	None observed
*RhoN19	Yes	None observed	Disruption of architecture/Blebbing
*Cdc42L61	Yes	Disruption of architecture	Disruption of architecture
*RacV12	Yes	Disruption of architecture	Disruption of architecture
*RhoV14	Yes	Disruption of architecture	Disruption of architecture
RhoWT	No	Not known	Not known
Par3 FL	No	Not known	Not known
Par3 PDZ1	No	Not known	Not known
Par3 PDZ2	Yes	None observed	None observed
Par3 PDZ3	Yes	Changes media color	Changes media color
Par6 FL	Yes	Not known	Not known
Par6 CT	No	Not known	Not known
Par6 NT	Yes	Not known	Not known

* Gift from Jonathan Chernoff FCCC.

Table 1. Summary of viral constructs generated, phenotypic observations in 3D cell culture system and traditional 2D cell culture system.

Protein Expressed	Successful Virus Generation	Phenotypic observation in 2D	Phenotypic observation in 3D	Activation of ErbB2 phenotype in 3D
Flag Par6 FL	Yes	EGF independent proliferation	EGF independent proliferation	Blebbing in late day structures
Par6 FL Flag	Yes	EGF independent proliferation	EGF independent proliferation	Blebbing in late day structures
FL Par6	No	Not known	Not known	Not known
Flag Par6 C-Terminal	Yes	None observed	None observed	Not known
Flag Par6 N-Terminal	No	Not known	Not known	Not known
Flag Par6 PDZ	Yes	None observed	None observed	Not known
Flag Par6 K19A	Yes	None observed	None observed	Blocks multistructures
Flag Par6 M235W	Yes	None observed	Not known	Not known
Flag Par6 ΔPro136	Yes	None observed	Not known	Not known
Flag FL Par6 β	Yes	EGF independent proliferation	EGF independent proliferation	Blebbing in late day structures

Table 2. Summary of retroviral constructs generated, phenotypic observations in 3D cell culture system and traditional 2D cell culture system.

Key Research Accomplishments:

- Determined that adenoviral mediated protein expression is a useful system to inducibly express proteins of interest in growth arrested 3D acini structures.
- Standardized conditions of adenoviral infection in MCF-10A cell line in 2D and 3D
    - Observation RhoN19 and RacN17 disrupt the development of 3D acini but do not disturb maintenance of structure once they have been formed.
- Determined conditions to express Rho family and activation of ErbB2 in 3D.
    - Observation that RhoN19 cooperates with ErbB2 to disrupt acini architecture.
- Generation of adenoviral vectors, adenovirus and retrovirus.
    - Adenoviral Vectors:
        - Par6 N-terminal
        - Par6 C-terminal
        - Par3 truncation PDZ1
        - RhoA wild type
    - Adenovirus:
        - Par3 truncation PDZ2
        - Par3 truncation PDZ3
        - Cdc42N17
        - RhoN19
        - Par6 full length
    - Retrovirus in MSCV IRES GFP:
        - Par6 full length
        - Par6 C-terminal
        - Flag Par6 PDZ
        - Flag Par6 K19A
        - Flag Par6 M235W
        - Flag Par6 ΔPro136
        - Flag FL Par6 β
- Generation of MCF-10A cell lines expressing Par proteins (see below)
- Determined that Par6 inducibly binds ErbB2
- Determined that Par6K19A mutation inducibly binds ErbB2
- Par6K19A expression inhibits ErbB2 induced multi-acinar phenotype without effecting reinitiation of proliferation
- Identified the ability of Par6 to promote EGF independent cell proliferation in 2D
- Identified the ability of Par6 to promote EGF independent cell proliferation in 3D
- Identified the ability of Par6 to promote Erk1/2 signaling

Reportable Outcomes:

Manuscripts:

Victoria Aranda, Teresa Haire, Marissa E. Nolan, Joseph P. Calarco, James P.Fawcett, Tony Pawson, and Senthil K. Muthuswamy, *Par6-aPKC uncouples ErbB2 induced disruption of epithelial organization and proliferation control* Accepted- Nat Cell Biol, 2006

Academic:

Successful defense of thesis proposal - March 2004

Oral presentation: **Stony Brook University Student Seminar**: Biological effects of activating distinct ErbB receptor dimers in polarized growth arrested epithelia. Nolan M, Muthuswamy SK -April 2004
Cold Spring Harbor Laboratory Student seminar: The role of Rho-GTPases in ErbB2 induced transformation of mammary epithelial acini- Nolan M, Muthuswamy SK - May 2004
Stony Brook University Student Seminar: Biological effects of Par6 over-expression in mammary epithelial cells- Nolan M, Basu S, Muthuswamy SK - January 2005
Cold Spring Harbor Laboratory Student seminar: Biological effects of Par6 over-expression in mammary epithelial cells- Nolan M, Basu S, Muthuswamy SK - February 2005

Poster presentation: **Stony Brook University Genetic Program Symposium**: Biological effects of activating distinct ErbB receptor dimers in polarized growth arrested epithelia Nolan M, Muthuswamy SK-January 2004
Stony Brook University Genetic Program Symposium: Biological effects of Par6 over-expression in mammary epithelial cells- Nolan M, Basu S, Muthuswamy SK - January 2005
Era of Hope Department of Defense Breast Cancer research Program Meeting: Biological effects of activating distinct ErbB receptor dimers in polarized growth arrested epithelia Nolan M, Muthuswamy SK- June 2005
The American Society for Cell Biology, 45th Annual Meeting: Biological effects of Par6 over-expression in mammary epithelial cells Nolan M, Basu S, Muthuswamy SK - December 2005
Stony Brook University Genetic Program Symposium: Biological effects of Par6 over-expression in mammary epithelial cells- Nolan M, Basu S, Muthuswamy SK - January 2006
Molecular mechanisms and Models of Cancer, CSHL: Biological effects of Par6 over-expression in mammary epithelial cells Nolan M, Basu S, Muthuswamy SK – August 2006

Development of reagents and cell lines:
Cell lines:
MCF-10A expressing C-Terminal Flag tag Par6 full length, high/medium/low expression
MCF-10A expressing C-Terminal Flag tag Par6 full length and ErbB2 chimera
MCF-10A expressing N-Terminal Flag tag Par6 full length high/medium/low expression
MCF-10A expressing N-Terminal Flag tag Par6 C-Terminal truncation
MCF-10A expressing N-Terminal Flag tag Par6 C-Terminal truncation and ErbB2 chimera
MCF-10A expressing N-Terminal Flag tag Par6 full length and ErbB2 chimera
MCF-10A expressing N-Terminal Flag tag Par6 PDZ truncation
MCF-10A expressing N-Terminal Flag tag Par6 PDZ truncation and ErbB2 chimera
MCF-10A expressing N-Terminal Flag tag Par6 K19A mutation
MCF-10A expressing N-Terminal Flag tag Par6 K19A mutation and ErbB2 chimera
MCF-10A expressing N-Terminal Flag tag Par6 Δpro136 mutation
MCF-10A expressing N-Terminal Flag tag Par6 Δpro136 mutation and ErbB2 chimera

MCF-10A expressing N-Terminal Flag tag Par6 M235W mutation
MCF-10A expressing N-Terminal Flag tag Par6 M235W mutation and ErbB2 chimera
MCF-10A expressing N-Terminal Flag tag Par6 β
MCF-10A expressing N-Terminal Flag tag Par6 β and ErbB2 chimera
MCF-10A expressing My-ER
MCF-10A expressing My-ER and N-Terminal Flag tag Par6 full length

Conclusion: Previously we have determined that ErbB2 activation re-initiates proliferation and disrupts cell polarity. First we have effectively characterized that ErbB2 initiated cell polarity disruption prior to initiating proliferation in growth arrested monolayers. Secondly, we have determined that ErbB2 recruits a functional Par complex and interfering with this complex abrogates multi-acinar formation without effecting proliferation. This study has separated ErbB2's ability to promote proliferation from epithelial cell architecture disruption.
We also observed cooperation between ErbB2 and dominant negative Rho, which further disrupts 3D acinar architecture. Lastly, overexpression of Par6 in mammary epithelial cells confers EGF independent proliferation in both 2D and 3D cell culture systems. The observed Par6 induced EGF independent growth phenotype may be of great relevance to understand the transformation process in polarized cells such as the mammary gland and thus we plan to focus on the characterization of this pathway. These studies may identify a novel signaling pathway by which oncogenes regulate cell polarity as well as new roles for polarity regulators in transformation.

References:

1. Yarden, Y. and M.X. Sliwkowski, *Untangling the ErbB signalling network.* Nat Rev Mol Cell Biol, 2001. **2**(2): p. 127-37.
2. Slamon, D.J., et al., *Studies of the HER-2/neu proto-oncogene in human breast and ovarian cancer.* Science, 1989. **244**(4905): p. 707-12.
3. Slamon, D.J., *Proto-oncogenes and human cancers.* N Engl J Med, 1987. **317**(15): p. 955-7.
4. Ohno, S., *Intercellular junctions and cellular polarity: the PAR-aPKC complex, a conserved core cassette playing fundamental roles in cell polarity.* Curr Opin Cell Biol, 2001. **13**(5): p. 641-8.
5. Humbert, P., S. Russell, and H. Richardson, *Dlg, Scribble and Lgl in cell polarity, cell proliferation and cancer.* Bioessays, 2003. **25**(6): p. 542-53.
6. Lemmers, C., et al., *hINADl/PATJ, a homolog of discs lost, interacts with crumbs and localizes to tight junctions in human epithelial cells.* J Biol Chem, 2002. **277**(28): p. 25408-15.
7. Hurd, T.W., et al., *Direct interaction of two polarity complexes implicated in epithelial tight junction assembly.* Nat Cell Biol, 2003. **5**(2): p. 137-42.
8. Stoll, M., et al., *Genetic variation in DLG5 is associated with inflammatory bowel disease.* Nat Genet, 2004. **36**(5): p. 476-80.
9. Nakagawa, S. and J.M. Huibregtse, *Human scribble (Vartul) is targeted for ubiquitin-mediated degradation by the high-risk papillomavirus E6 proteins and the E6AP ubiquitin-protein ligase.* Mol Cell Biol, 2000. **20**(21): p. 8244-53.
10. Qiu, R.G., A. Abo, and G. Steven Martin, *A human homolog of the C. elegans polarity determinant Par-6 links Rac and Cdc42 to PKCzeta signaling and cell transformation.* Curr Biol, 2000. **10**(12): p. 697-707.

11. Eder, A.M., et al., *Atypical PKCiota contributes to poor prognosis through loss of apical-basal polarity and cyclin E overexpression in ovarian cancer.* Proc Natl Acad Sci U S A, 2005. **102**(35): p. 12519-24.
12. Regala, R.P., et al., *Atypical protein kinase Ciota plays a critical role in human lung cancer cell growth and tumorigenicity.* J Biol Chem, 2005. **280**(35): p. 31109-15.
13. Regala, R.P., et al., *Atypical protein kinase C iota is an oncogene in human non-small cell lung cancer.* Cancer Res, 2005. **65**(19): p. 8905-11.
14. Sahai, E. and C.J. Marshall, *RHO-GTPases and cancer.* Nat Rev Cancer, 2002. **2**(2): p. 133-42.
15. Fritz, G., I. Just, and B. Kaina, *Rho GTPases are over-expressed in human tumors.* Int J Cancer, 1999. **81**(5): p. 682-7.
16. Lin, R., et al., *A novel Cdc42Hs mutant induces cellular transformation.* Curr Biol, 1997. **7**(10): p. 794-7.
17. Zondag, G.C., et al., *Oncogenic Ras downregulates Rac activity, which leads to increased Rho activity and epithelial-mesenchymal transition.* J Cell Biol, 2000. **149**(4): p. 775-82.
18. Mira, J.P., et al., *Endogenous, hyperactive Rac3 controls proliferation of breast cancer cells by a p21-activated kinase-dependent pathway.* Proc Natl Acad Sci U S A, 2000. **97**(1): p. 185-9.
19. Muthuswamy, S.K., M. Gilman, and J.S. Brugge, *Controlled dimerization of ErbB receptors provides evidence for differential signaling by homo- and heterodimers.* Mol Cell Biol, 1999. **19**(10): p. 6845-57.
20. Muthuswamy, S.K., et al., *ErbB2, but not ErbB1, reinitiates proliferation and induces luminal repopulation in epithelial acini.* Nat Cell Biol, 2001. **3**(9): p. 785-92.
21. Simpson, K.J., A.S. Dugan, and A.M. Mercurio, *Functional analysis of the contribution of RhoA and RhoC GTPases to invasive breast carcinoma.* Cancer Res, 2004. **64**(23): p. 8694-701.

Appendix I: Supporting Data

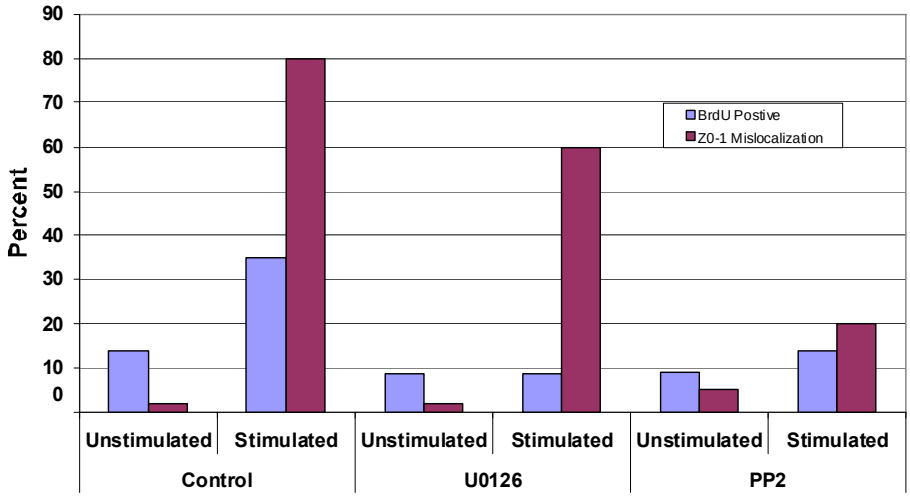

Figure 1. Inhibition of the Src Kinase (PP2) pathway prevents mislocalization of Z0-1. While inhibition of MAPK (UO126) pathway reduces proliferation while Z0-1 is still mislocalized. MDCK cells expressing ErbB2 were activated with or without inhibitor (1uM) for 15 hours. BrdU incorporation or ZO-1 localization was quantitated by immunofluoresence.

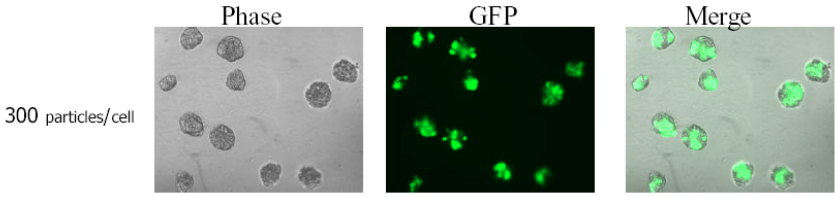

Figure 2. Expression of control GFP Virus in polarized, growth arrested acini structures. MCF-10A cells were grown until Day 12, infected with GFP virus and allowed to express for 4 days. Image taken on D16.

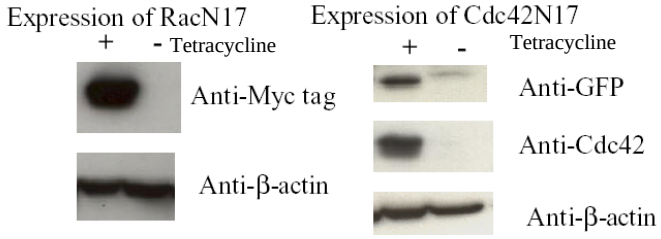

Figure 3. Tetracycline regulated expression of cdc42N17 and RacN17 in 3D lysate. MCF-10A cells were grown until Day12, infected with or without tetracycline and lysed on Day16

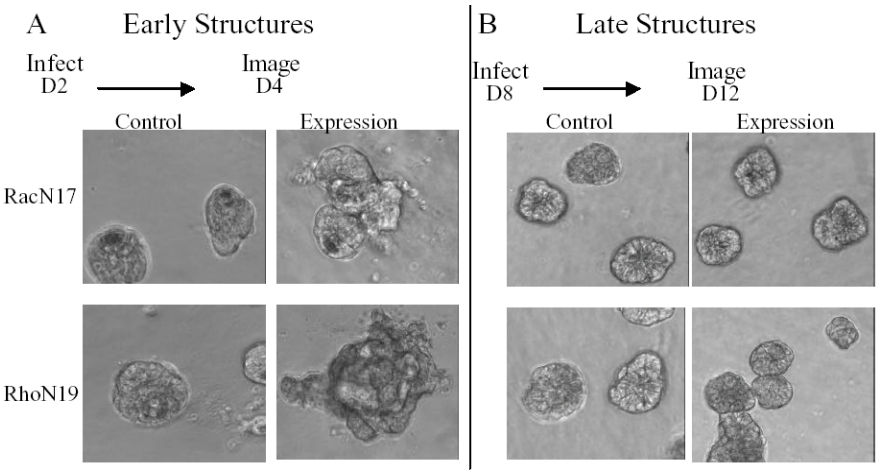

Figure 4. Infection of RacN17 and RhoN19 at different time points of acini development. Both proteins affect development of acini structures (A). However neither protein affects the structure once they are established (B). Acini were either infected from Day 2 and imaged on Day4 or infected on Day 8 and imaged on Day 12.

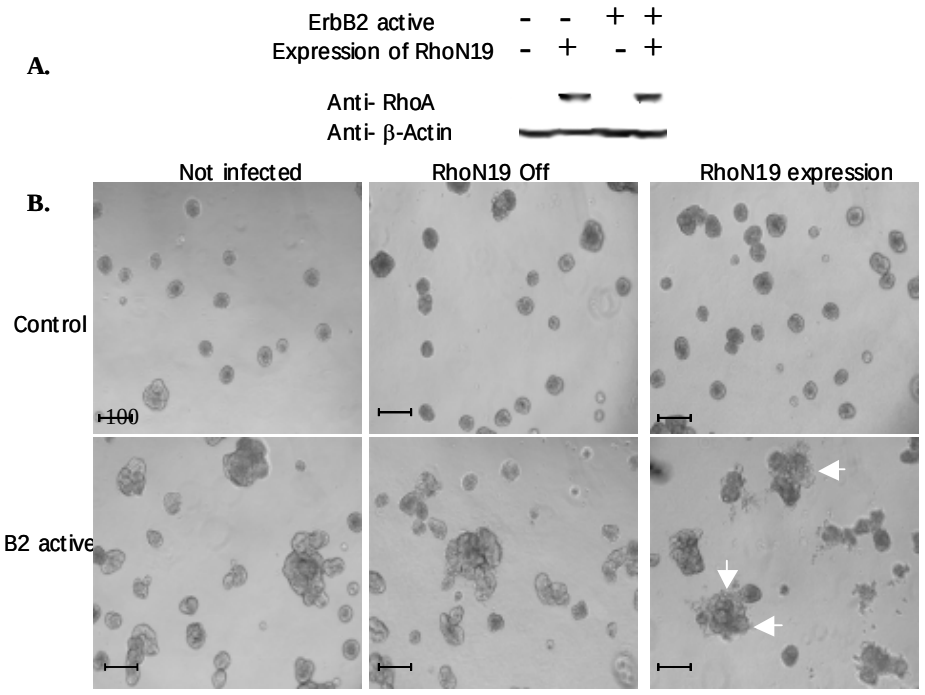

Figure 5. Activation of ErbB2 in cooperation with RhoN19 expression further disrupts acinar morphology. A) RhoN19 expression in 3D acini lysate. B)Typical presentation of multi-structure phenotype in dimerized ErbB2 without RhoN19 expression (Bottom,left panel). "Blebs" of cells extending from the main body are observed upon expression of RhoN19 RhoN19 expression and ErbB2 activation cooperate to further disrupt acini architecture (Bottom right panel). Acini were infected on Day 12 and ErbB2 was activated in the presence or absence of tetracycline for 4 days.

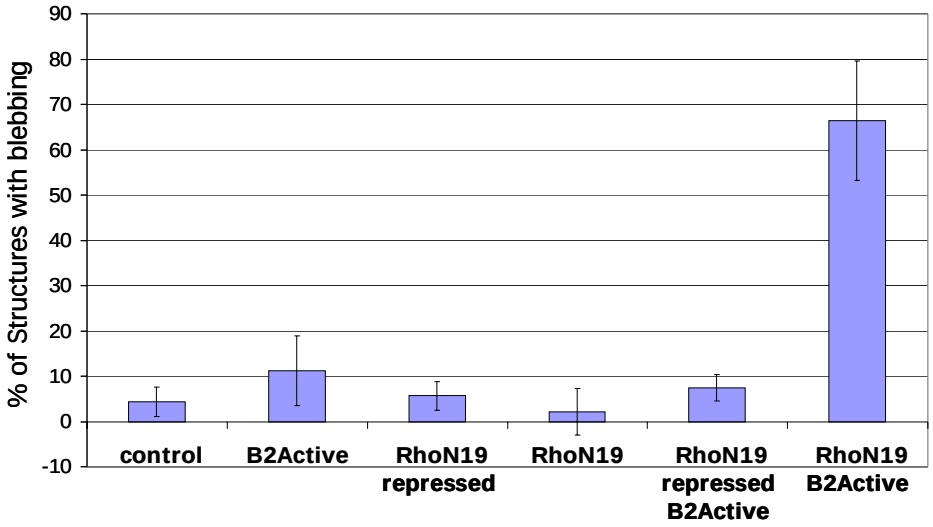

Figure 6. Quantification of dimerized ErbB2 and RhoN19 induced blebbing phenotype in mammary epithelial cells in Figure 5.

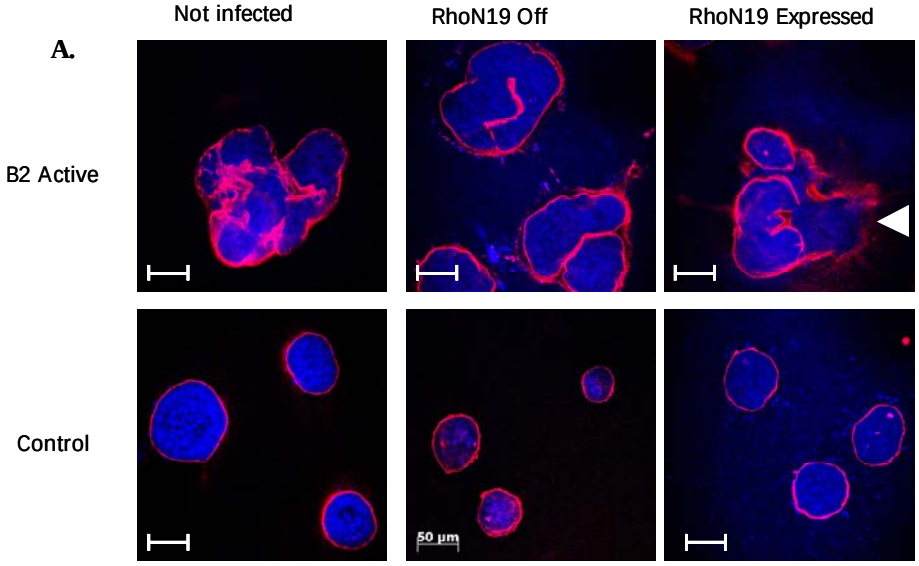

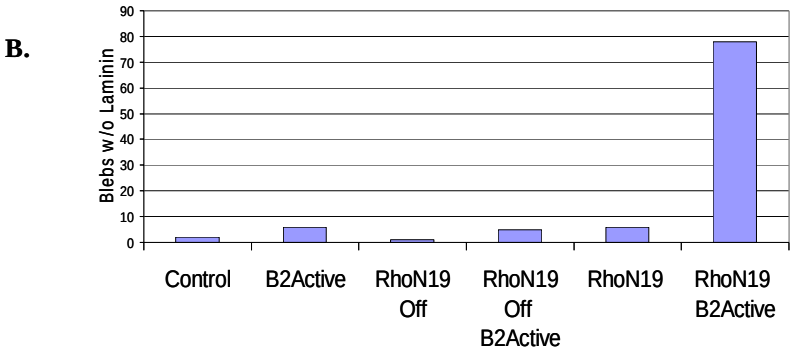

Figure7. Acini expressing RhoN19 with activated ErbB2 lack organized laminin. A) Immunofluorecent staining of acini with DAPI (blue) and laminin (red). There is a lack of a laminin border around acini upon ErbB2 activation and RhoN19 expression. . B) Quantification of "blebbing" phenotype without organized laminin under ErbB2 dimerization and RhoN19 expression conditions.

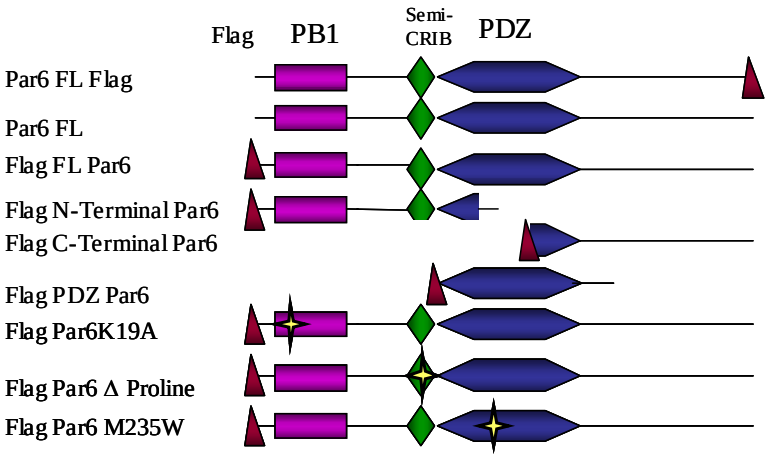

Figure 8. Par6α Constructs in MSCV IRES GFP

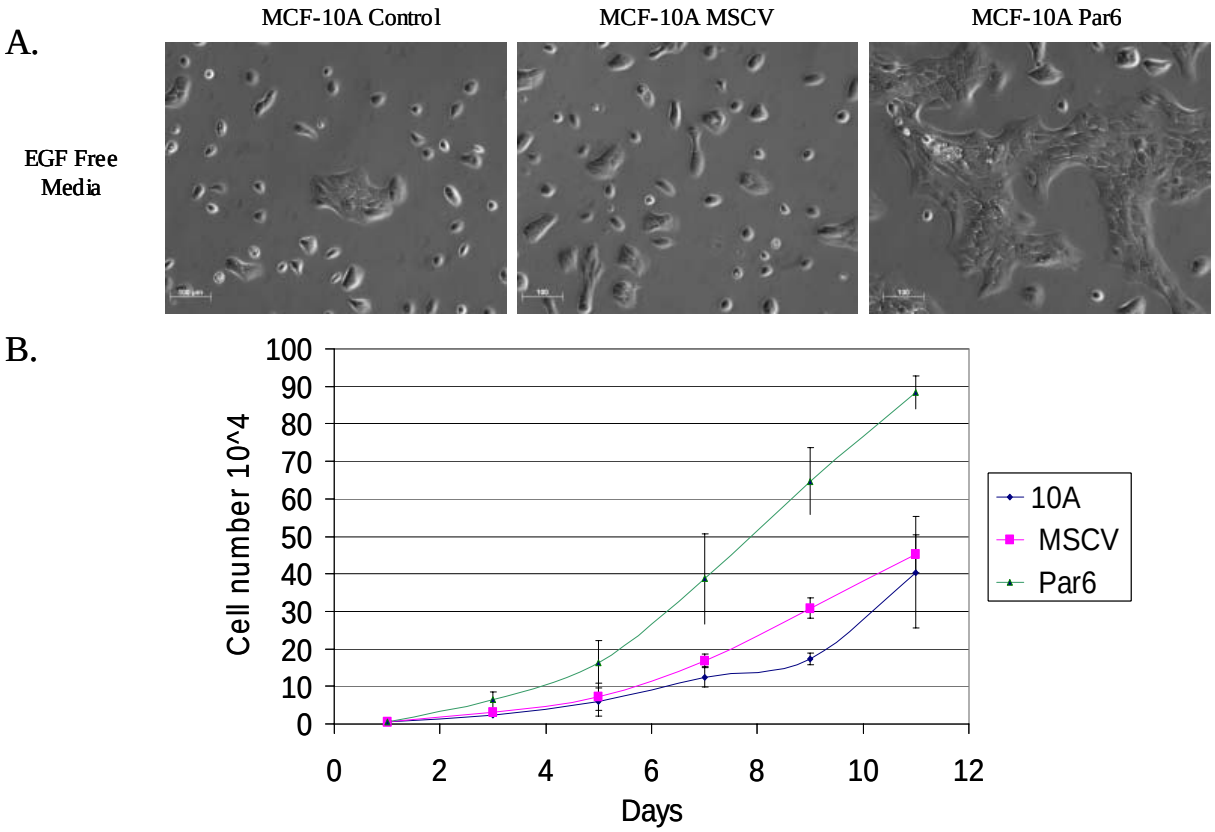

Figure 9. Par6 overexpression results in EGF independent proliferation. A) Phase-contrast image of cells on Day 3 in EGF free media. B) 10A, control MSCV and Par6 (10,000) cells were grown over a period of 11 days in EGF free media. Cells were harvested every other day, counted and cell numbers were plotted

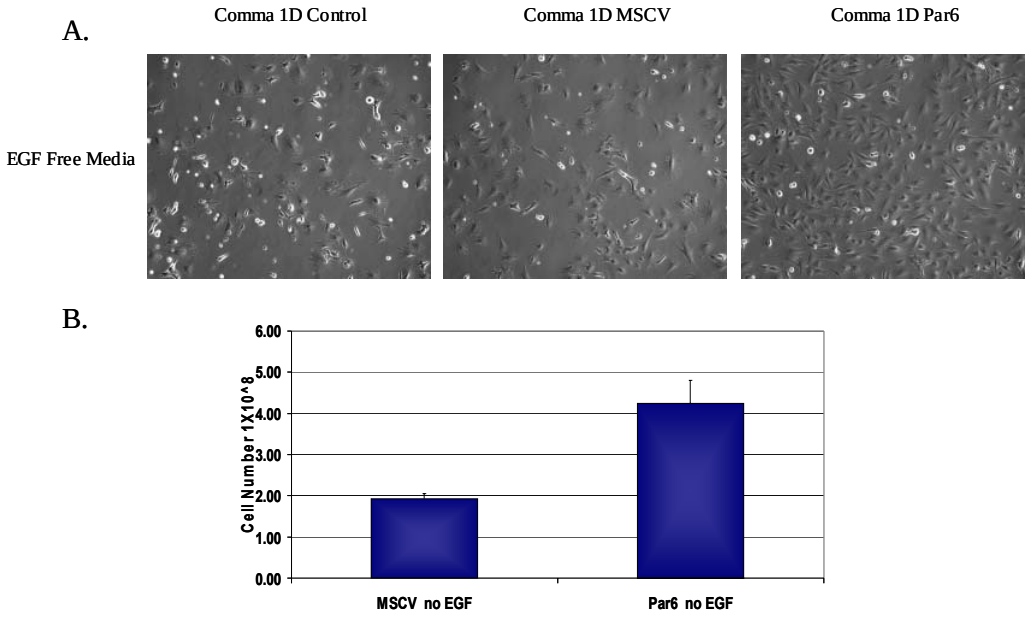

Figure 10. Phenotypic verification in mouse mammary epithelial cell line (comma 1D). A) Phase contrast images of comma 1D cells in EGF free media. B) Proliferation of comma D cells in EGF free media as monitored by cell number. Comma 1D cells over-expressing Par6 grow independent of EGF.

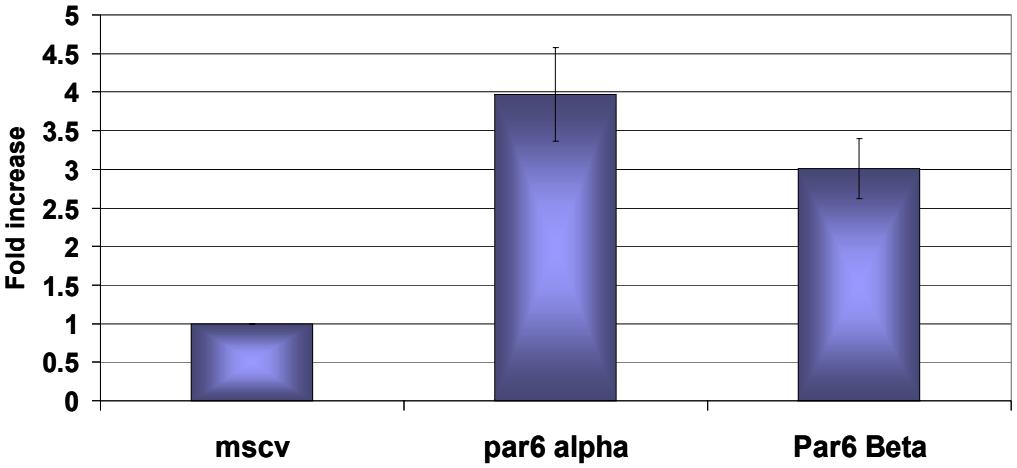

Figure 11. Multiple isoforms of Par6 promote EGF independent proliferation. Comparison of S-phase, represented in fold increase of Par6 over-expressing cells in s-phase compared to MSCV control cells. Cells were plated on day 0, 30% media changed on day 1 and fixed on day 3. Cells were stained with propidium iodide and samples were run on BD LSRII flow cytometer. Percentage of cells in S-phase was calculated using ModFit.

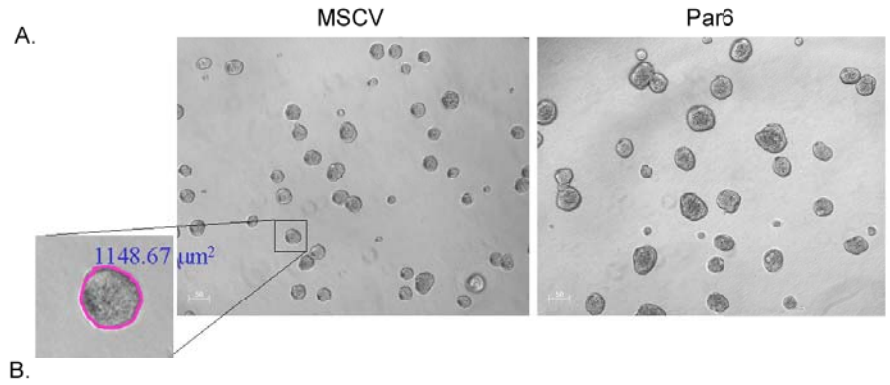

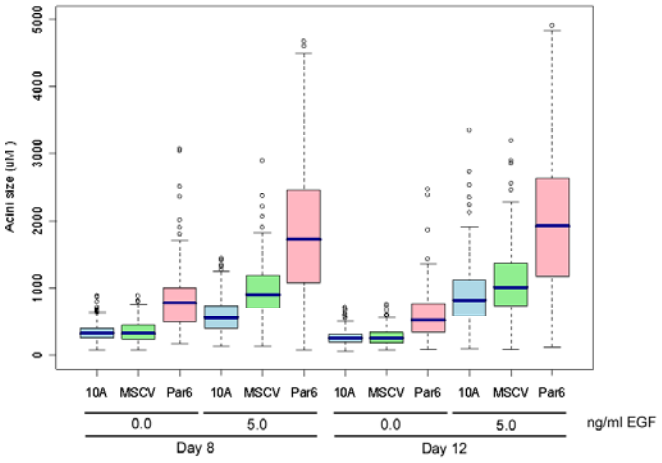

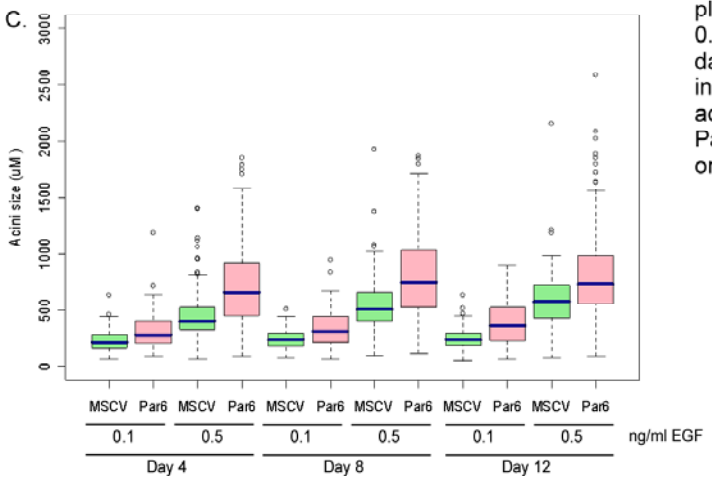

Figure 12. Par6 overexpression promotes acini morphogenesis. A) Phase image of Day 12 acini structures. These structures are growth arrested and have a polarized architecture with a single layer of epithelium surrounding a lumen. B) Cells were plated on matrigel in the presence of or absence of 5 ng/ml EGF and grown for 12 days. Phase contrast images were taken every 4 days. The area of each acini was quantitated using imaging software from Zeiss. The acini size distribution is plotted as a box plot. The box outlines 50% of the data with the median value drawn as a blue line. The data represents more than 200 individual acini structures. The difference in acini size distribution between MSCV and Par6 is very significant on Day8, Day12 with $P<0.001$. C) Par6 cooperates with low dose EGF to promote acini morphogenesis. Cells were plated on matrigel in the presence of 0.01 or 0.05 ng/ml EGF (low dose) and grown for 12 days. The data represents more than 200 individual acini structures. The difference in acini size distribution between MSCV and Par6 with 0.05ng/ml EGF is very significant on Day 4, 8, and 12 with $P<0.001$.

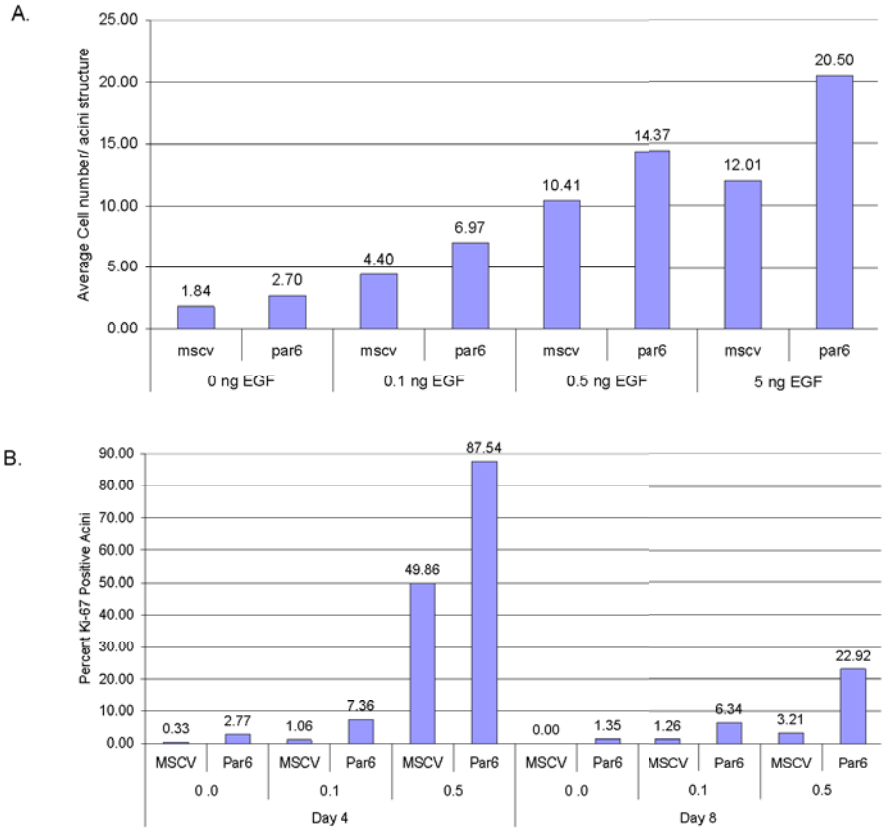

Figure 13 Par6 overexpression promotes acinar morphogenesis by increasing proliferation and acini cell number. A) Day 4 structures were stained with Dapi to observe the nuclei of the cell within the acini. Each cell was counted in each acini and graphed as average cell number/acini structure B) Day 4 and Day 8 structures were immunostained with Ki-67 a cell proliferation marker. Acini structures that contained a positive Ki-67 cells were counted and the percent of acini structures with positive cells were graphed. For each experiment over 200 acini were counted.

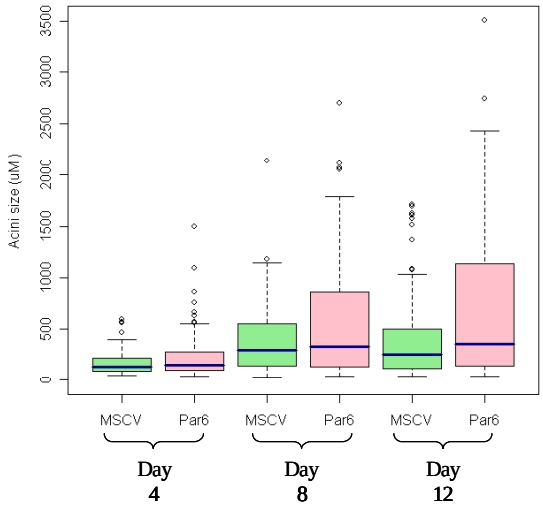

Figure 14. Par6 over-expressing cooperates with low does EGF to promote acini morphogenesis in a murine mammary epithelial cell line (HC11). Single cells were plated on matrigel in the presence of 0.05 ng/ml EGF and grown for 12 days. Phase contrast images were taken every 4 days and the area of each acini were quantitated. The acini size distribution is plotted as a boxplot. The box outlines 50% of the data with the median value drawn as a blue line. The data represents 100 individual acini structures from one experiment.

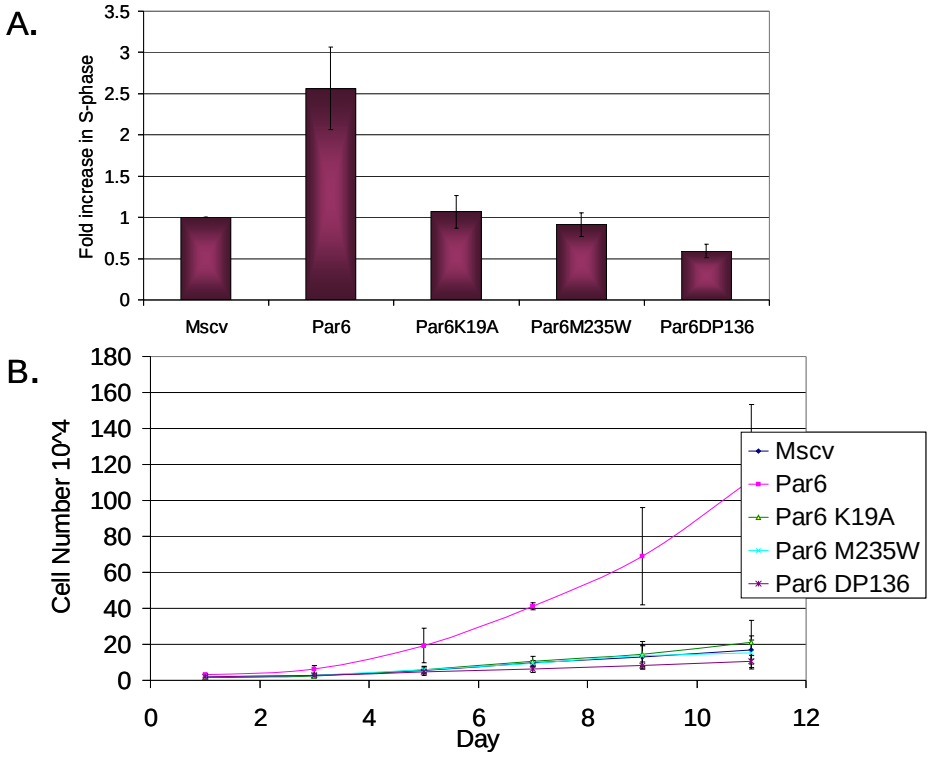

Figure 15. Par6 induced EGF independent proliferation requires aPKC and it's effectors. A) S-phase assay was performed as described in Figure 2 with control, Par6, Par6^{K19A}, Par6^{M235W} and Par6$^{\Delta pro136}$. These par6 mutations do not promote EGF independent proliferation. B) Control and mutant Par6 cells were plate and grown over a period of 11 days in EGF free media. Cells were harvested every other day, counted and cell numbers were plotted.

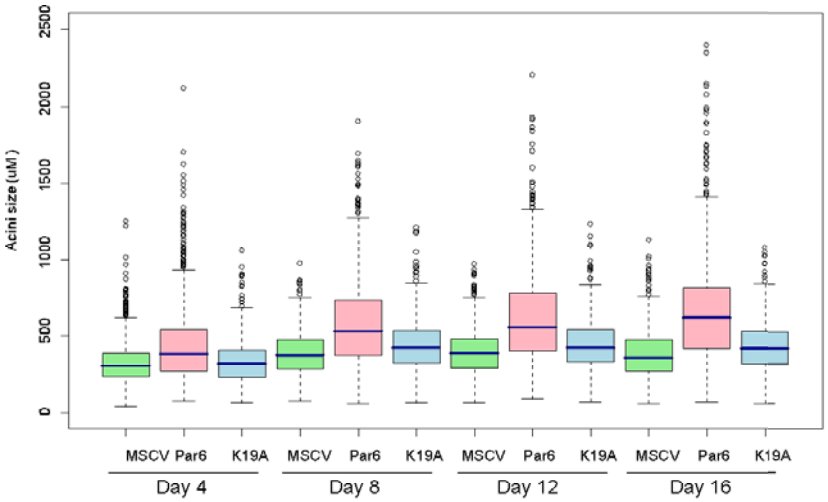

FIgure 16. Par6 over-expressing cooperates with low does EGF to promote acini morphogenesis while overexpression of mutatn Par6K19A does not promote proliferation. The area of each acini was quantitated using imaging software from Zeiss. The acini size distribution is plotted as a box plot. The box outlines 50% of the data with the median value drawn as a blue line. The data represents more than 800 individual acini structures from three independent experiments. The difference in acini size distribution between MSCV and Par6 is very significant on Day4, Day8 and Day 12 with P<0.001. There is no significant difference between MSCV and K19A.

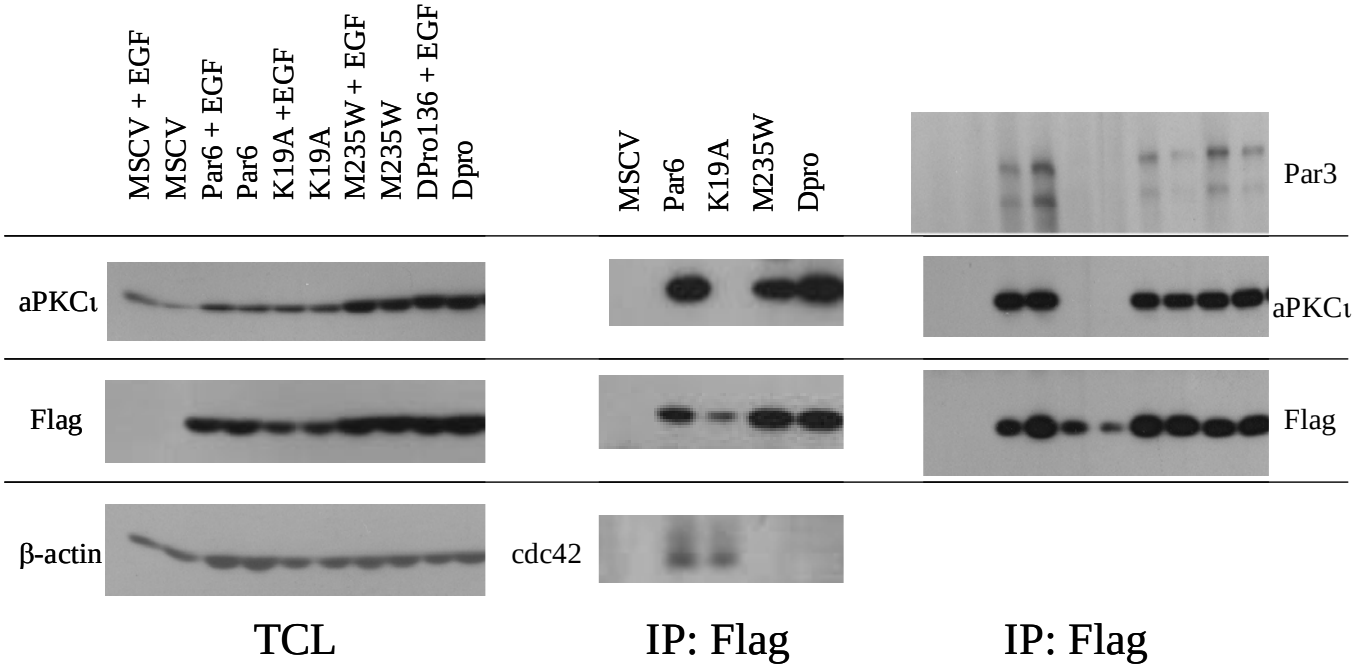

Figure 17. Par6 mutations are deficient in binding Par complex. Immunoprecipitations of flag tagged par6 mutations show that Par6K19A is deficient in binding aPKC, and that Par6ΔPro136 is deficient in binding Cdc42.

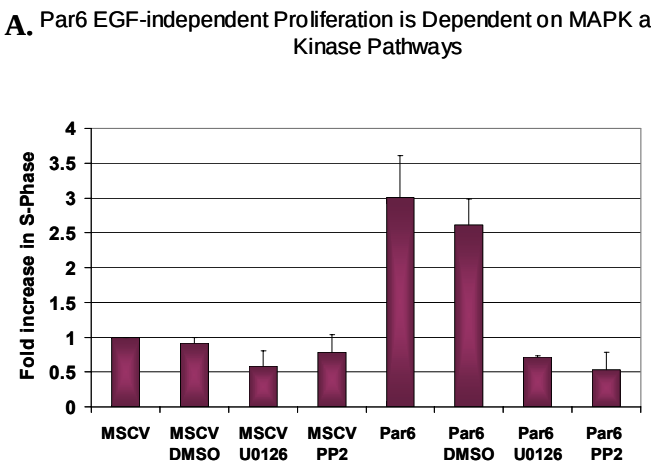

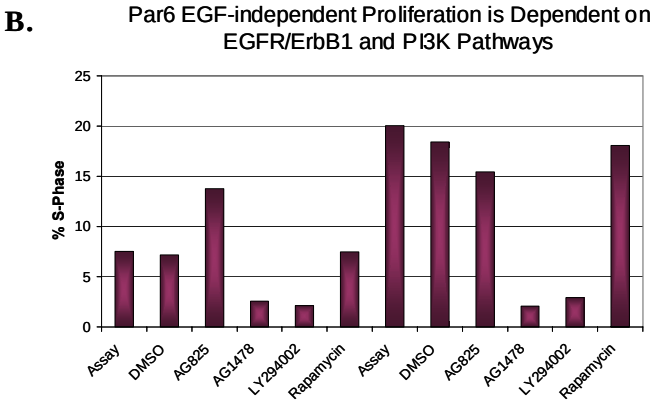

Figure 18. A) Inhibition of Src, MAPK and B) PI3K signal transduction pathways prevents EGF independent proliferation in Par6 cells. B) Inhibition EGFR kinase activity inhibits proliferation but inhibition of ErbB2 and MTOR doesn't affect increase in S-phase.

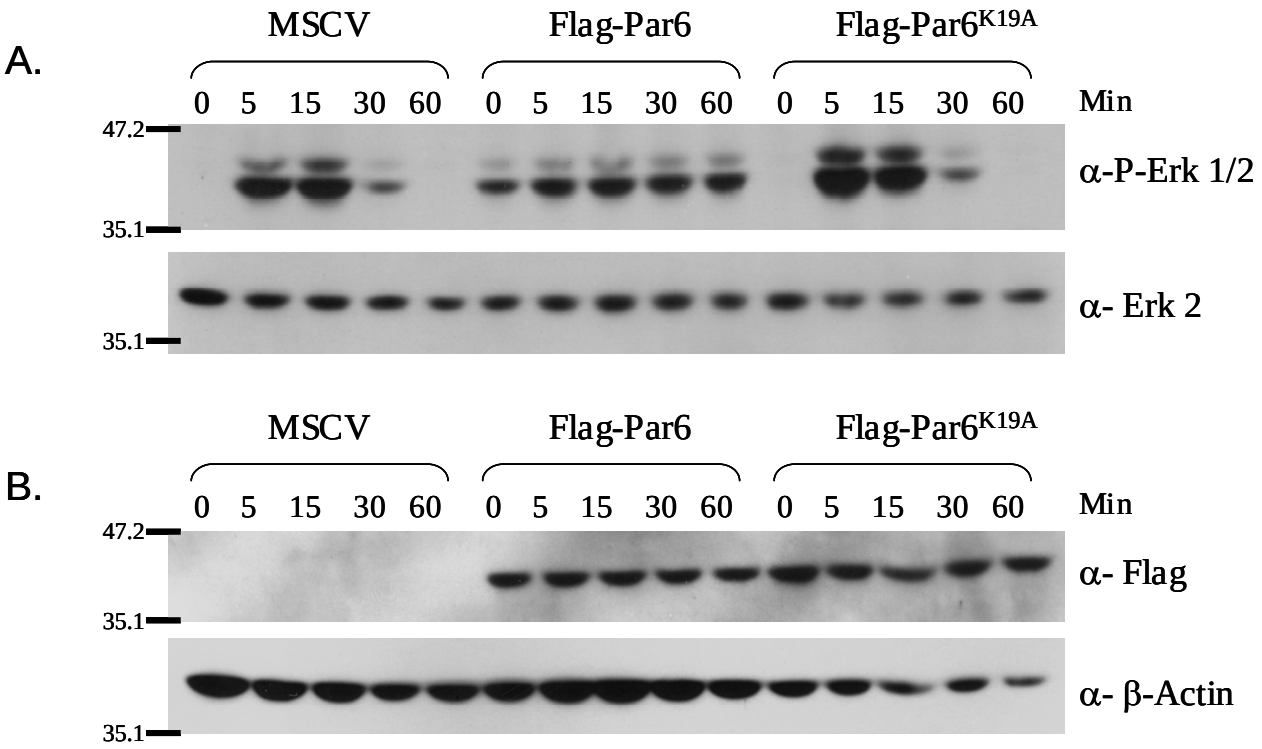

Figure 19. Par6 over-expression but not MSCV or Par6^{K19A}, sustains ERK1/2 phosphorylation. Par6 expression also increased basal phospho-ERK1/2. A) MSCV, Par6 and Par6^{K19A} cells were deprived of growth factors for 24 hour and stimulated with 2ng/ml EGF for a time course of 5,15,30, 60 minutes. Lysates were collected and analyzed for phosphorylated ERK1/2 by western analysis. B) Western analysis showing equal levels of par6 and mutant

Appendix II: Abstracts

Era of Hope Department of Defense Breast Cancer research Program Meeting - June 2005

THE BIOLOGICAL EFFECTS OF ACTIVATING ERBB2 RECEPTOR TYROSINE KINASE IN POLARIZED GROWTH ARRESTED MAMMARY EPITHELIA

Marissa E. Nolan[1,2] and Senthil K. Muthuswamy[1]
[1]Cold Spring Harbor Laboratory, Cold Spring Harbor, NY, [2] Genetics Program, Stony Brook University, Stony Brook, NY

Malignant breast cancer appears to develop over time from mammary epithelial cells that have been transformed. These transformed cells form early lesions that are characterized by uncontrolled proliferation and loss of epithelial architecture. The receptor tyrosine kinase ErbB2/HER2 is over-expressed in 25-35% of breast cancers and correlates with poor clinical prognosis. We are interested in understanding the molecular mechanisms by which ErbB2 contributes to early lesion formation and progression.

Our lab combines a unique system to study the inducible effects of ErbB2 receptor with a three-dimensional cell culture system. ErbB2 receptors have the ability to homo and heterodimerize generating a complex signaling system. We have circumvented this problem by generating a chimeric ErbB2 that homodimerizes upon addition of synthetic ligand to generate specific downstream signals. We are also culturing mammary epithelial cells (MECs) on a matrigel matrix. The cells form three-dimensional acini-like structures with a single layer of epithelial cells surrounding a luminal space. These structures have characteristics similar to the resting epithelium of mammary glands, such as low proliferation rate and organized architecture. Previously, we have shown that activation of ErbB2 in MECs re-initiates proliferation and disrupts cell polarity resulting in a multi-acinar phenotype. Our studies have suggested a possible role of Rho GTPase and that Par complex, a key regulator of cell polarity, in ErbB2 induced phenotype.

The Rho family of small GTPase (RhoA, Rac1, CDC42) is overexpressed in breast cancer. They are involved in cell polarity as well as in proliferation and migration pathways. Although there is no direct link between ErbB2 and Rho, some studies link activation of ErbB signaling to Rho regulations. I am investigating the involvement of the Rho pathways in ErbB2-induced disruption of human mammary epithelial acini. Inhibition of Rac and Cdc42 utilizing a dominant negative (N17T) mutation did not inhibit the ErbB2 phenotype. Surprisingly, inhibition with RhoN19T cooperates with ErbB2 activation. The 3D structures are further disrupted by protrusions and blebbing formations. Currently, we are characterizing this phenotype to determine if the structures are invasive. We also want to determine the molecular mechanisms involved in this signaling pathway.

The Par complex is known to regulate cell polarity, which is one of the aspects of cellular architecture that is disrupted in cancer. This complex consists of Par6, aPKC, Par3 and Cdc42/Rac1. We have observed that overexpression of Par6 promotes EGF independent proliferation in 2D cell culture. We are characterizing the function of the Par complex in the polarized mammary epithelial cells, and its possible implication in ErbB2 induced disruption.

Understanding how these proteins affect proliferation and cell polarity and their relationship to Erbb2 will identify diagnostic markers and drug targets to treat breast cancer.

The American Society for Cell Biology, 45th Annual Meeting - December 2005

Biological effects of Par6 over-expression in mammary epithelia

Marissa E. Nolan[1,2], Srinjan Basu[1] and Senthil K. Muthuswamy[1]
[1]Cold Spring Harbor Laboratory, Cold Spring Harbor, NY, [2] Genetics Program, Stony Brook University, Stony Brook, NY

Mammary epithelial cells line the ducts of the mammary gland and possess apical-basal asymmetry, referred to as cell polarity. This is essential for epithelial function and it is also thought to play a role in growth control of resting tissue. Recent studies have identified three protein complexes, the Par3/Par6/aPKC complex, Scribble/Lgl/Dlg complex and the Crumbs/PALS1/PATJ complex that act in a hierarchal manner to establish cellular architecture. However, regulation of apical-basal polarity in other contexts such as disease is poorly understood. As loss of epithelial cell architecture and re-initiation of proliferation are common features of early hyperplastic lesions, it is becoming increasingly important to decipher the underlying molecular mechanisms that initiate disruption of apical-basal polarity.

Recent evidence suggests that alterations in the polarity machinery may contribute to oncogenesis. Loss of LKB1 (Par4) and Dlg5 are predisposition factors for human cancer and the human papillomavirus protein E6, targets scribble for degradation. It has also been shown that Par6 cooperates with RacV12 to transform fibroblasts.

Par6 is thought to play an important role in connecting the structural components of the polarity machinery with cellular signaling pathways. Through its PDZ and CRIB domains it interacts with aPKC, Par3 and CDC42. In addition, Par6 has been shown to interact with Crumbs and Scribble complexes. It is not well understood how these interactions are regulated to provide the multiple functions of Par6.

In order to investigate Par6 function in the context of polarized epithelia, we use a non-transformed mammary epithelial cell line (MCF-10A). MCF-10A cells require exogenous EGF for growth and form acini with distinct architecture when cultured on collagen and laminin. We are using both the 3D cell culture system and tradition cell culture to investigate the biological and signaling effects of Par6 overexpression in MCF-10A cells.

Mechanisms and Models of Cancer, Cold Spring Harbor Laboratory - August 2006

BIOLOGICAL EFFECTS OF PAR6 OVER-EXPRESSION IN MAMMARY EPITHELIA

Marissa E. Nolan[1,2], Srinjan Basu[1] and Senthil K. Muthuswamy[1]
[1]Cold Spring Harbor Laboratory, Cold Spring Harbor, NY, [2] Genetics Program, Stony Brook University, Stony Brook, NY

Mammary epithelial cells line the ducts of the mammary gland and possess apical-basal asymmetry, referred to as cell polarity. Recent studies have identified three protein complexes, the Par3/Par6/aPKC complex, Scribble/Lgl/Dlg complex and the Crumbs/PALS1/PATJ complex that act in a hierarchal manner to establish apical-basal polarity. Recent evidence suggests that alterations in the polarity machinery may contribute to oncogenesis. Loss of LKB1 (Par4) and Dlg5 are predisposition factors for human cancer and the human papillomavirus protein E6, targets scribble for degradation. It has also been shown that Par6 cooperates with RacV12 to transform fibroblasts.

Whether the polarity proteins regulate process other than cell architecture is not well understood. In our efforts to study the effect of deregulating the function of Par protein complex in human mammary

epithelial cells, we made an unexpected observation: overexpression of Par6 induced growth-factor independent proliferation of mammary epithelial cells.
Overexpression of Par6 induced epidermal growth factor-independent proliferation of human mammary epithelial cell line, MCF-10A, grown on plastic culture dishes and promoted EGF-independent morphogenesis of MCF-10A cells in three-dimensional culture. Overexpression of Par6 also cooperated with low doses of EGF to promote proliferation in 3D acini. However, Par6 did not cooperate with EGF to induce migration demonstrating that not all EGF-induced effects are regulated by Par6 overexpression. Consistent with the effect of inducing proliferation, Par6 overexpression resulted in constitutive ERK activation in the absence of EGF, and cooperated with EGF to promote sustained ERK activation. Thus I have identified a new role for polarity proteins as mediators of EGF-induced cell proliferation.

Appendix III: Biographical sketch

BIOGRAPHICAL SKETCH

NAME	POSITION TITLE
Marissa Nolan	Graduate Student

EDUCATION/TRAINING *(Begin with baccalaureate or other initial professional education, such as nursing, and include postdoctoral training.)*

INSTITUTION AND LOCATION	DEGREE *(if applicable)*	YEAR(s)	FIELD OF STUDY
Sacred Heart University, CT	B.S.	1999	Biology
Stony Brook University, NY	Ph.D. Program	2001-Present	Genetics

A. Positions and Honors

Employment

May 1998-May 1999 — Laboratory Intern, American Diagnostica, Greenwich, CT
Developed a novel enzyme linked immunosorbent assay (ELISA) for the quantitation of activated FVII in plasma and biological fluids

June 1999-August 2001 — Assistant Scientist, American Diagnostica, Greenwich, CT
Developed four novel ELISA's for blood coagulation and fibrinolytic proteins; began a project to develop a system to target breast cancer cells that over-express urokinase plasminogen activating receptor (UPAR) utilizing different recombinant proteins *in vivo*

Experience

Fall 1996-Spring 1997 — Undergraduate Research at Sacred Heart University, CT
Investigated the structure and function of stress response genes in *Dictyostelium discoideum* (Dd) and their role in protecting the Dd amoebae from stress-induced damage

September 2001-November 2001 — Graduate Rotation Student in the laboratory of Dr. Arthur Grollman, Stony Brook University, NY
Cloning, expression and purification of DNA polymerase to examine the role of pol t's in DNA repair and mutagenesis

December 2001-February 2002	Graduate Rotation Student in the laboratory of Dr. Scott Lowe, Cold Spring Harbor Laboratory, NY Developed a retroviral vector that utilized cre-mediated recombination to reversibly express genes in primary cell lines
March 2002-Present	Graduate Student in the laboratory of Dr. Senthil Muthuswamy, Cold Spring Harbor Laboratory, NY Studying the biological effects of activating distinct ErbB receptor dimers in polarized growth arrested epithelia
August 2003-2004	Student Representative, Watson School of Biological Sciences Executive Committee, Cold Spring Harbor Laboratory, NY
September 2004-January 2006	Student Representative, Genetics Program Executive Committee, Stony Brook University, NY

Honors

1995, 1997, 1998	Sacred Heart University Trustee Scholarship
August 16, 2003-	Department of Defense Breast Cancer Fellowship (DAMD17-03-01-0193)
August 15, 2006	"The biological effects of activating distinct ErbB receptor dimers in polarized growth arrested epithelia"
January 2006	Distinguished service award, Stony Brook University Genetics Program, Stony Brook, NY

B. Selected peer-reviewed publications (in chronological order)

Victoria Aranda, Teresa Haire, Marissa E. Nolan, Joseph P. Calarco, James P.Fawcett, Tony Pawson, and Senthil K. Muthuswamy, *Par6-aPKC uncouples ErbB2 induced disruption of epithelial organization and proliferation control* Accepted- Nat Cell Biol, 2006

Appendix IV: Manuscript

NCB-M09679A-A

Par6-aPKC uncouples ErbB2 induced disruption of epithelial organization and proliferation control@

Victoria Aranda[1]#, Teresa Haire[1,2]#, Marissa E. Nolan[1,3], Joseph P. Calarco[4,6], James P. Fawcett[5], Tony Pawson[5], and Senthil K. Muthuswamy[1,2,3,4]*

[1]Cold Spring Harbor Laboratory, [4]Watson School of Biological Sciences, One Bungtown Road, Cold Spring Harbor, NY, 11724, [2]Department of Molecular Genetics and Microbiology, [3]Graduate Program in Genetics, Stony Brook University, NY, 11794.

[5]Program in Molecular Biology and Cancer, Samuel Lunenfeld Research Institute, Mount Sinai Hospital, 600, University Avenue, University of Toronto, Toronto, Ontario, M5G 1X5, Canada

[6]Department of Chemistry, University of Toronto, 80 Saint George St. Toronto M5S 3H6, Canada

# These authors contributed equally to this work

*Corresponding author

One Bungtown Road

Cold Spring Harbor Laboratory

Cold Spring Harbor

New York

11724

Phone: 516 367 6975

Fax: 516 367 8461

E-mail: muthuswa@cshl.edu

@ We dedicate this work to the memory of our friend and colleague, Teresa Haire.

Summary:

The loss of tissue organization is a defining feature of all carcinomas, which are cancers of epithelial origin. Luminal epithelial cells in normal glands are organized as single layers with apical-basal polarity. This organization is lost early during neoplastic transformation. Here, for the first time, we identify a mechanism used by oncogenes to disrupt epithelial organization. Activation of ErbB2, an oncogenic receptor tyrosine kinase, initiated disruption of epithelial architecture at the apical-lateral border that progressed to a loss of apical polarity. ErbB2 directly recruited and regulated Par6-aPKC, a polarity complex that controls establishment of apical-lateral border. Interfering with the ability of ErbB2 to recruit functional Par6-aPKC blocked ErbB2-induced disruption of epithelial organization in a three dimensional organotypic culture system. In the absence of ErbB2-Par6-aPKC, ErbB2 retained its ability to induce proliferation, which resulted in increased apoptosis. Blocking apoptosis failed to completely rescue the disruption in epithelial organization suggesting a unique role of Par complex in mediating changes in organized epithelia. Thus, we identify a novel arm of oncogenic signaling that uses polarity regulators to disrupt epithelial organization and is distinct from pathways that control apoptosis and cell proliferation.

The defining features of carcinoma are increase in proliferation and loss of tissue architecture. Although both normal glands and cancerous lesions have proliferating epithelial cells, epithelia in normal glands retain glandular organization, which is lost in cancerous lesions.[1]. Many studies have identified mechanisms by which oncogenes that initiate carcinoma induce proliferation, but we know little about how they signal to disrupt epithelial organization. In addition to cancer, abnormal tissue architecture is observed in disease states such as chronic inflammation[2], which increases the risk of cancer[3]. Thus, understanding the mechanisms by which oncogenes deregulate epithelial organization is of significant biological importance.

Glandular epithelia in organs such as the breast have apical, lateral and basal surfaces -- a modular organization referred to as apical-basal polarity[4]. While apical membranes are rich in microvilli, lateral membranes have cell-cell junctions and the basal surfaces have cell-matrix adhesions[4]. Whereas the boundary between the lateral and basal membranes is undefined, the border between apical and lateral membrane is defined by the presence of tight junctions. The tight junctions are made up of transmembrane proteins such as occludins, claudins and junctional adhesion molecules and cytoplasmic proteins such as Zonula Occludens 1 (ZO-1)[5]. This glandular organization is an evolutionarily conserved feature that regulates vectoral secretion of milk into the luminal space, a critical function of normal mammary gland.

Many oncogenes implicated in carcinoma*,* when overexpressed in epithelial cells in culture*,* induce changes in epithelial cell morphology and organization. For instance, we and others have previously shown that activation of oncogenes such as ErbB2[6], K-ras[7], Raf[8], Fos[9], Jun[10], Rho and Rac[11], CDC42[12] and v-Src[13] in epithelial cells disrupts polarity and organization by affecting localization of apical membranes and tight junctions. However, the mechanism by which this happens is not known, in part, due to our poor understanding of the events that regulate development of normal epithelial cell polarity.

Studies using model organisms such as *D. melanogaster* and *C. elegans,* and more recently using mammalian epithelia, have led to the identification of a set of evolutionarily conserved proteins collectively referred to as polarity regulators. These proteins direct establishment and maintenance of normal epithelial organization and function[14,15]. The polarity regulators are broadly grouped as the Crumbs complex, the Scribble complex and the Par complex, and their concurrent action directs the establishment of apical-basal asymmetry in developing epithelia[14,15]. Recently, alteration of polarity regulators, such as mutations in Dlg5, has been correlated with disruption of epithelial organization observed in patients inflammatory bowl disease[16]. Although loss of epithelial organization is an early event in carcinoma, the possible

role of polarity regulators in oncogene-mediated transformation of epithelial cells has never been addressed.

Here, we investigate how oncogenic signaling by ErbB2, a receptor tyrosine kinase, disrupts epithelial organization. We chose ErbB2 because it is overexpressed or amplified in 25 –30% of breast cancers and is also implicated in other epithelial malignancies associated with organs such as ovary, prostate, pancreas and the salivary gland[17,18]. We have previously shown that culturing the non-tumorigenic mammary epithelial cell line, MCF-10A in a three dimensional (3D) matrix results in formation of proliferation arrested epithelial structures that resemble mammary acini *in vivo* [6]. These structures have a single layer of epithelial cells surrounding a hollow central lumen. Activation of ErbB2 in 3D organized structures induces uncontrolled proliferation and disrupted epithelial organization resulting in formation of large multiple-acini-like non-invasive structures [6]. These large structures have their luminal space filled with proliferating cells that have low rates of apoptosis and as a whole resemble hyperplastic outgrowth.

The ErbB2 phenotype contrasts with those promoted by other oncogenes such as cyclin D1, which fail to give rise to hyperplastic outgrowths but induce uncontrolled proliferation that is coupled to increased rates of apoptosis. Co-expression of cyclin D1 and an anti-apoptotic protein Bcl2, induces uncontrolled proliferation and protects cells from apoptosis, but still does not generate the hyperplastic outgrowth observed after activation of ErbB2. This suggests that a combination of increased rates of proliferation and decreased apoptosis is not sufficient to disrupt 3D organization of epithelial cells. Thus, ErbB2 must use distinct mechanisms to deregulate epithelial organization, which together with increased proliferation and decreased rates apoptosis result in disruption of 3D organization that resembles hyperplastic outgrowth.

Here we demonstrate that activation of ErbB2 initiates disruption of cell architecture by directly interacting with the Par polarity complex. Inhibition of the functional interaction between ErbB2 and the Par complex blocks the ability of ErbB2 to disrupt epithelial organization but does not interfere with the increase in proliferation thereby uncoupling oncogene-induced proliferation from oncogene-induced changes in epithelial organization. Our results define a role for epithelial polarity regulators in oncogenesis by uncovering a novel aspect of ErbB2 signaling that regulates epithelial architecture.

RESULTS

Activation of ErbB2 in polarized epithelia induced disruption of apical polarity

In order to understand the effect of activating ErbB2 on apical-basal polarity, we expressed a synthetic ligand-inducible form of ErbB2 receptor[19] in a cell line that can establish a polarized monolayer in culture-- the Madin-Darby Canine Kidney II (MDCK II) cells[20]. Activation of ErbB2 signaling in these cells, using a small molecule dimerizing ligand referred to as AP1510[21] (dimerizer), induced an increase in receptor tyrosine phosphorylation (Suppl. Fig. 1A) and activation of downstream signaling molecules such as Erk (data not shown). MDCK cells expressing ErbB2 were allowed to form confluent, polarized monolayers by plating them on porous transwell filters. Polarized monolayers formed in the absence of dimerizer displayed normal apical-basal polarity as monitored by asymmetric localization of apical polarity markers, glycoprotein 135 (gp135) and GM130, a lateral membrane marker, Epithelial(E)-cadherin and a apical-lateral border marker, tight junction-associated protein, ZO-1 (Figure 1A and Suppl. Fig. 1B). Activation of ErbB2 induced disruption of apical-basal polarity as monitored by re-localization of gp135 and ZO-1 to the lateral membrane (Fig. 1A) and by loss of apical orientation of the Golgi apparatus (Suppl. Fig. 1B). In addition, oncogenic signaling by ErbB2 induced re-initiation of proliferation (Fig. 1D) and promoted formation of regions of multilayered epithelia, where the basally located layers of cells were surrounded by cell-cell junctions and lacked any detectable apical surface (Suppl. Fig. 1B).

ErbB2-induced changes in apical-basal polarity were reversed upon removal of dimerizer (Suppl. Fig. 2A) correlating with downregulation of ErbB2 receptor phosphorylation. Moreover, neither short term (1 day) nor long-term (7 days) activation of ErbB2, induced expression of mesenchymal markers such as vimentin (data not shown), suggesting that ErbB2-induced changes represent an early oncogene-dependent stage of the transformation process. Thus, activation of ErbB2 in polarized epithelial cells induced disruption of epithelial organization and loss of apical polarity and serves as a model for the changes observed in early lesions *in vivo*.

ErbB2-induced disruption of polarity initiates at apical-lateral border

In order to dissect how oncogenes disrupt apical polarity, we first determined the temporal order by which oncogenic signaling by ErbB2 affects cell polarity. Using markers that distinguish apical, lateral and apical-lateral border, we determined that apical proteins and the apical-lateral border marker, ZO-1, were restricted to a 3.0 μm region from the cell apex (Fig. 1B and Suppl.

Fig 3A) in polarized monolayers. ZO-1 was never observed in optical sections that were 4.0 μm from the cell apex (Suppl. Fig 3A). During the first 30 minutes of ErbB2 activation, the tight junction associated protein ZO-1 was detected in optical sections that were 4.0 – 5.0 μm from the apex of the cell, without any detectable presence of apical membrane protein gp135 (Fig. 1B, Suppl. Fig 3A). However, prolonged activation (2 - 4 hrs) also resulted in mislocalization of gp135 (Fig 1B), which was followed by initiation of cell cycle (8 – 12 hrs) (Fig. 1D) and formation of multilayered epithelial sheets (10 - 18 hrs) (Fig. 1C). Thus, ErbB2-induced disruption of polarized organization initiated at tight junctions and progressed towards a loss of apical polarity and epithelial organization.

To determine whether ErbB2 activation specifically altered ZO-1 localization or broadly affected proteins at the apical-lateral border, we monitored changes in distribution of other proteins known to localize to that region of the cell[5]. Transmembrane proteins such as occludins, junctional adhesion molecule, and cell junction-associated proteins such as Rab5, and AF-6, were also mislocalized upon activation of ErbB2 (data not shown). In addition, there was an increase in the permeability of tight junctions as determined using fluorescently labeled Dextran (10,000 MW) (Suppl. Fig. 2B). Thus, the effect of activating ErbB2 was not restricted to ZO-1, but resulted in a structural and functional disruption of multiple proteins at the apical-lateral border. These observations suggest that ErbB2 may disrupt the apical-lateral border not by targeting junctions specifically, but rather by affecting the molecular machinery that regulates establishment and maintenance of polarized organization in epithelial cells.

ErbB2 activation disrupts Par complex

The Par complex, composed of scaffolding proteins Par3 and Par6, the atypical protein kinase C (aPKC) and small GTP binding proteins, CDC42/Rac1, is the critical regulator of establishment and maintenance of tight junctions located at the apical-lateral border [22-25]. We analyzed the localization of Par6 in MDCK.ErbB2 cells that stably express flag-tagged Par6. In unstimulated monolayers, Par6 concentrates at the apical-lateral border membrane, but upon ErbB2 activation this localization is lost (Fig. 2A), suggesting that ErbB2 activation affects the Par complex.

The composition of the Par complex is regulated during tight junction biogenesis[22-25]. In epithelial cells that are induced to loose cell-cell contacts by incubation in calcium-free media, Par6-aPKC exists in a complex independent of Par3 and CDC42 [26]. Formation of cell-cell

junctions, by repletion of calcium, is thought to trigger binding of GTP-bound CDC42 to Par6-aPKC and increase the aPKC activity. Par3 is subsequently recruited to Par6-aPKC-CDC42 to form the 'active' Par complex, which regulates formation of junctions at apical-lateral border[22-25]. Since our results demonstrate that ErbB2 induces functional and structural disruption of tight junctions, we asked whether ErbB2 affects the composition of Par polarity complex. Activation of ErbB2 induced a more than two-fold decrease in the levels of Par3-aPKC association but did not affect the interaction between aPKC and Par6 (Fig.2D and 2E) suggesting that ErbB2 regulates the Par complex by disrupting Par3 from Par6-aPKC complex. Neither Par3 nor Par6 were tyrosine phosphorylated upon activation of ErbB2 (data not shown), suggesting that they were not direct substrates of ErbB2 kinase activity. Interestingly, ErbB1/EGFR a related receptor tyrosine kinase that lacks the ability to disrupt polarity[6] did not affect the interaction between the members of the Par complex (data not shown) suggesting that the ability to disrupt Par complex may be related to the ability of the oncogene to disrupt apical-basal polarity.

ErbB2 forms a physical complex with Par6-aPKC

Although the role played by Par complex during oncogene-induced disruption of cell polarity is not known, a recent study demonstrated that Par6 plays a critical role during TGFβ-induced epithelial-mesenchymal transition, where TGFβ receptor type-1-bound Par6 is required for a RhoA-dependent disruption of tight junctions[27]. We asked whether ErbB2 interacts with the Par complex to mediate its effect on epithelial cell polarity. Among the members of Par complex, Par6-aPKC, but not Par3, associated with activated ErbB2 (Fig. 2B, 2C), suggesting ErbB2 recruits Par6-aPKC but not Par3. The ability of Par6-aPKC to associate with ErbB2 was detected within 15 minutes of receptor activation and sustained thereafter (Fig 2B and data not shown). Unlike TGFβR1-Par6 interaction, which does not require ligand binding, ErbB2-Par6 interaction requires receptor dimerization suggesting that Par6-aPKC may utilize distinct mechanisms to interact with cell surface receptors.

Taken together, these results suggest that oncogenes such as ErbB2 directly regulate the Par polarity complex and disrupt junctional complexes at the apical-lateral border and thus regulate epithelial architecture.

The ability of ErbB2 to recruit functional Par6-aPKC is required for disruption of organized epithelial acini

Next we wanted to use the information gained on how ErbB2 disrupts apical-basal polarity to understand how ErbB2 disrupts epithelial organization in 3D organized epithelia. To this end, we have previously demonstrated that a non-transformed human mammary epithelial cell line, MCF-10A, undergoes a morphogenetic program that gives rise to three dimensional (3D) acini-like structures with a single layer of polarized epithelial cells surrounding a hollow-central lumen, when cultured over a layer of extracellular matrix[6]. Moreover, we have also demonstrated that inducible activation of ErbB2 in 3D acini-like structures results in re-initiation of proliferation and formation of hyperplastic structures that have an abnormal multi-acinar organization with filled lumens[6], providing a context to interrogate the molecular mechanisms by which signaling by ErbB2 disrupts epithelial organization.

As observed in MDCK cells, activation of ErbB2 in MCF-10A cells coexpressing ErbB2 and flag-tagged Par6 induced recruitment of Par6-aPKC to the receptor (Fig. 3A). Based on this observation, we investigated whether the ability of ErbB2 to recruit Par6-aPKC is required for its ability to disrupt epithelial organization. Atypical PKC is recruited to the Par complex by virtue of its ability to bind PB1 domain in Par6 and is a critical mediator of Par complex function[23,25]. Par6-aPKC interaction is required for promoting assembly of active Par complex and expression of kinase-dead aPKC interferes with polarization of epithelial cells [28]. We hypothesized that a Par6 mutant that does not interact with aPKC can dominantly interfere with the ability of ErbB2 to signal through the Par complex. As expected, the Par6 Lys 19 to Ala (Par6K19A) mutant that does not bind aPKC[29,30] bound to ErbB2 but failed to recruit aPKC to the receptor complex (Fig. 3A) when expressed in 10A.ErbB2 cells. Next, we compared the effects of activating ErbB2 in cells expressing wt Par6 with those expressing Par6K19A using the 3D morphogenesis assay.

Whereas activation of ErbB2 induced an increase in the number of hyperplastic structures in control and wild type Par6 expressing cells, it was significantly defective in cells that express Par6K19A (Fig. 3B and 3C). In order to avoid any sampling bias induced by counting hyperplastic structures, we measured the area of 3D structures before and after ErbB2 activation (see Material and Methods), and analyzed the data for quantitative differences in acini populations (Fig. 3D). Activation of ErbB2 in parental or wild type Par6 expressing cells induced a significant change in the distribution of acini size around the median value (Fig. 3D), whereas activation of ErbB2 in cells expressing Par6K19A did not dramatically alter the distribution of acini size (Fig. 3D). Statistical analysis using two-way analysis of variance (ANOVA) for interaction between the gene expressed and the effect of ErbB2 activation, demonstrated a significant interaction between ErbB2-induced effect in Par6K19A cells and parental or Par6

expressing cells (Table 1). The effect of expressing Par6K19A was specific to ErbB2 induced changes because it did not affect epidermal growth factor (EGF)-induced normal morphogenesis (Figure 3B, 3D and Table 1). Thus, we have demonstrated that the interaction between ErbB2 and Par6-aPKC is critical for ErbB2-induced disruption of 3D epithelial acini.

ErbB2-Par6-aPKC pathway is not required for ErbB2-induced proliferation

In addition to its ability to disrupt 3D organized epithelia[6], ErbB2 is a potent inducer of cell proliferation[31]. As such, we asked whether the ErbB2 induced effects on cell proliferation and organization were under same or distinct genetic/biochemical pathways. To this end, we investigated whether the ability of ErbB2 to promote proliferation was affected in cells expressing Par6K19A. Interestingly, ErbB2 induced an increase in proliferation in Par6K19A expressing cells similar to that of control or wild type Par6 expressing cells grown in 3D cultures (Fig. 4A). To confirm that this is not restricted to cells grown in 3D context, we analyzed Par6K19A expressing cells under normal plastic 2D culture conditions to determine the ability of ErbB2 activation to promote EGF-independent proliferation. In these conditions, activation of ErbB2 potently induced proliferation in the presence of Par6K19A suggesting that Par6-aPKC recruitment was not required for the ability of ErbB2 to promote proliferation (Fig. 4B). While previous studies have identified the Ras-Raf pathway as a critical mediator of ErbB2-induced proliferation[31], our results identify the Par6-aPKC pathway as the critical mediator of ErbB2-induced effect on epithelial organization. Thus, we have uncovered a new branch of ErbB2´s oncogenic signaling that uncouples proliferation and epithelial organization control, and is required for transformation of 3D organized epithelial cells.

Inhibition of apoptosis in Par6K19A cells is not sufficient to rescue ErbB2 induced effects

We have previously demonstrated that cell located in the middle of the MCF-10A acinus undergo apoptosis during development of luminal space[32]. ErbB2 induced formation of large hyperplastic structures with filled lumens is related to its ability to induce proliferation and block apoptosis[6,32]. The ability of Par6K19A mutant to block ErbB2 induced formation of hyperplastic structures while retaining ErbB2 induced proliferation control prompted us to analyze changes in apoptosis and filling of the luminal space. While activation of ErbB2 in cells expressing wild type Par6 correlated with low levels of apoptosis, we observed high levels of apoptosis upon ErbB2

activation in Par6K19A expressing cells (Fig. 5A). In addition, ErbB2 activation induced filling of luminal space in 3D acini derived from wild type Par6 expressing cells whereas ErbB2 activation failed to fill lumens in structures derived from Par6K19A cells (Fig. 5B). Thus, the increased apoptosis may be responsible for the inability of ErbB2 to induce formation of hyperplastic structures in Par6K19A cells. The increase in apoptosis in the presence of Par6K19A was apparent only when cells were grown as 3D structures (data not shown) suggesting that epithelial organization is required to reveal the relationship between ErbB2, Par complex and apoptosis.

To directly test the role played by increased apoptosis in the ability of Par6K19A to block ErbB2 induced disruption of 3D acini, we expressed an anti-apoptotic protein Bcl2 in Par6K19A cells (Fig. 6A). Consistent with our previous studies that Bcl2 blocks apoptosis in 3D acini [32], expression of Bcl2 inhibited the increase in apoptosis observed in ErbB2 activated Par6K19A cells (Fig 6C). However, ErbB2 activation still failed to form large, hyperplastic structures at the same levels as Par6 expressing cells upon ErbB2 activation (Fig. 6B). Blocking apoptosis only partially rescues the ErbB2 induced phenotype in Par6K19A cells as activation of ErbB2 in Par6K19A.Bcl2 cells induced formation of 30% multiacinar structures which contrast the 42% multiaciniar structures observed for Par6.Bcl2 cells (Fig 6D). Furthermore, the hyperplastic structures formed in Par6K19A.Bcl2 were significantly smaller than those formed in wild type Par6.Bcl2 cells upon activation of ErbB2 (Fig. 6B). These results suggest that Par6-aPKC interaction with the receptor elicits unique signaling pathways that regulate epithelial organization.

Thus we identify polarity regulators as targets for oncogenic signaling that contribute to transformation independently of proliferation and survival control.

DISCUSSION

In this study we demonstrate a role for the polarity proteins, Par6-aPKC, in ErbB2-induced transformation of 3D organized epithelial structures. ErbB2 directly interacts and regulates the Par6-aPKC polarity complex. Whereas Par6-aPKC recruitment is not required for ErbB2-induced regulation of cell proliferation, it is necessary for disruption of cell organization. Thus, we have identified an arm of oncogenic signaling that is critical for disruption of epithelial organization, but is distinct from pathways that control cell proliferation.

Our results demonstrate that oncogene induced changes in cell proliferation and cell architecture can be uncoupled. This observation is supported by previous studies that identify the GTP binding protein Rac1 [33] and Signal Transducer and Activator of Transcription 3 (STAT3) [34] as required for disruption of cell polarity in transformed epithelia. How the Rac and STAT3 initiated pathways regulate epithelial cell polarity, independent of their ability to control proliferation [35,36] is unclear. Our present study provides a direct insight. We demonstrate that oncogenes disrupt cell and tissue organization by regulating polarity proteins that control establishment and maintenance of normal architecture in epithelia. Thus, while the well-established Ras-mitogen activated protein kinase pathway controls cell proliferation during ErbB2-induced oncogenesis[18,37], we identify the Par complex as a regulator of cell architecture during ErbB2 induced transformation of epithelial cells.

Our results also rise the possibility that disruption of polarity regulators can divert normal proliferative signals to those that induce aberrant growth. Consistent with this possibility, loss-of-function mutation of polarity genes promotes uncontrolled proliferation and abnormal tissue architecture in Drosophila[14]. A recent study provides the possibility that this hypothesis may also be true in mammals. Genetic variations in Dlg5, a polarity regulator gene, are associated with inflammatory bowl disease, which increases the risk of gastric cancer[3,16] suggesting that disruption of polarity regulators can sensitize the tissue for hyperproliferation and disrupted tissue organization, both properties observed in inflammatory disease. The above observations taken together, suggest that loss of cell polarity can either function as an initiating event or as a cooperating event during the multi-step progression of carcinogenesis.

Disruption of polarity may also function as a rate-limiting step during tumorigenesis. Consistent with this notion, we observed that in the absence of an interaction with functional Par complex, ErbB2 induced increase in cell proliferation was coupled to an increase in apoptosis. The

relationship between aberrant proliferation and apoptosis was observed in 3D organized epithelia, but not in cells grown as monolayer cultures suggesting that proper 3D organization reveals novel relationships between oncogene induced proliferation and control of cell death[32]. These observations have led us to propose that cell architecture can function as a 'checkpoint' during transformation of 3D organized epithelia, and the inability to disrupt it counteracts the transformation process by promoting cell death.

Studies on viral oncogenesis provide additional support to the notion that targeting cell polarity regulators is required for oncogenesis. The oncogenic functions of the high-risk human papillomavirus type 16, in the cervical cancers, map to the E6 and E7 genes[38]. Whereas E7 targets the tumor suppressor retinoblastoma protein, E6 mediates degradation of another tumor suppressor p53[39]. Several reports have suggested a p53-independent function for E6, which was subsequently related to the ability E6 to mediate degradation of polarity proteins Scribble and Dlg[40,41]. Mutants of E6 that lack the ability to degrade polarity proteins, but retain its ability to degrade p53, were defective in transforming cells[41], suggesting that the ability to disrupt cell architecture is a processes selected-for during the evolution of oncogenic tumor virus.

Our study also provides a novel insight into an old problem: Why is proliferation induced by oncogenic signaling result in a loss of tissue organization *in vivo*, but the proliferation induced by physiological signals retain normal tissue organization? It is possible that physiological stimuli, such as pregnancy, induce cell proliferation but retain normal tissue organization by promoting the function of polarity regulators that control tissue re-modeling. In contrast, oncogenes such as ErbB2 coordinately induce proliferation and disrupt regulators of tissue re-modeling, such as polarity proteins, which results in abnormal tissue architecture. Since disruption of tissue architecture is rarely observed in adult tissues but observed in almost all types of carcinoma, polarity pathways may identify targets that are unique to diseased organs/tissues[42]. Thus, understanding the mechanisms by which oncogenes disrupt polarity may provide a new therapeutic opportunity.

It is possible that the targets of the ErbB2-Par6-aPKC pathway will provide new opportunities for treating ErbB2 positive breast cancers. During establishment of cell polarity, Par6-aPKC regulates phosphorylation of Lgl, Par3, GSK3β and members of the Crumbs polarity complex to form proper apical-basal polarity [22-25], suggesting that targets of aPKC are regulators of aberrant cell architecture in ErbB2 induced tumors. Atypical PKC targets may not only be specific to ErbB2 positive cancers because recent observations demonstrate that aPKC is overexpressed in ovarian and NSCL carcinoma, and correlates with poor clinical prognosis[43,44]. Increased

expression of aPKC promoted loss of polarity and increased proliferation in ovarian epithelia[44] and a small molecule inhibitor of aPKC inhibited proliferation of NSCL cancer cells[45] highlighting a role for aPKC in cancer. Further analyses of this pathway may not only identify novel therapeutic targets but also identify novel diagnostic markers for carcinoma.

In this manuscript, we report that ErbB2 induced transformation of organized epithelia not only requires proliferative and anti-apoptotic stimuli but also requires a signal to disrupt cell architecture. This signal is provided by a direct interaction between ErbB2 and the Par polarity complex and loss of this interaction inhibits ErbB2 induced disruption of organized epithelia. Thus, we identify a novel pathway used by oncogenes to disrupt epithelial organization, which is critical for their oncogenic function. In doing so, we define a role for polarity proteins as mediators of oncogenic signaling that initiate epithelial malignancies.

Materials and Methods.

Materials. Antibodies: ZO1, Ki67 and JAM-1 (Zymed, San Francisco, CA); β-catenin, aPKCi, pTyr, AF-6; GM130 (BD Biosciences, San Jose, CA); mPar6 (Santa Cruz Biotechnology, Santa Cruz, CA); hPar6c antibody was generated against a N-terminal peptide sequence (MARPQRTPARSPDSI) in rabbits. HA (Covance, Princeton, NJ), mPar3 (Upstate Biotechnology, Lake Placid, NY); aPKCς (Santa Cruz Biotechnology), aPKCi (Transduction labs), cleaved caspase-3 (Cell Signaling Technology, Danvers, MA); gp135 (gift from James Nelson); Flag M2 (Sigma); Bcl-2 (Santa Cruz Biotechnology); Alexa Fluor conjugated secondary antibodies were from Molecular Probes, Eugene, OR. Dimerizer, AP1510 (ARIAD Pharmaceuticals, Cambridge, MA).

DNA Constructs. Construction and characterization of chimeric ErbB2 that can be activated by addition of a small molecule ligand, AP1510 (ARIAD Pharmaceuticals, Cambridge, MA) was previously described [19]. Carboxy or amino-terminal FLAG-tagged mouse par6C was generated by PCR amplification of mPar6C from pFLAG CMV mpar6C [46] and cloned into MSCV-PURO-IRES-GFP. cDNA for a kinase dead version of aPKCz (kindly provided by Cindy Miranti) was subcloned into MSCV-PURO-IRES-GFP (Kindly provided by Scott Lowe). MSCV-PURO-IRES-GFP vector for Bcl-2 expression was also kindly provided by Scott Loew. Preparation of virus, infection and selection were performed as described previously [6,47].

MDCK derived cell lines. MDCK cells were grown in Minimal Essential Medium (MEM, GibcoBRL, Grand Island, NE) supplemented with 10% fetal bovine serum, 50U/ml penicillin, 50u/ml streptomycin, and 50U/ml non-essential amino acids. Populations of Madin Darby Canine Kidney II cells expressing ErbB2 chimera (MDCK-ErbB2) were generated as described [6]. Clones expressing equal levels of the ErbB2 chimera were selected by anti-HA immunoblots and their ability to undergo dimerizer (AP1510)-inducible phosphorylation was determined as described previously [19]. MDCK-ErbB2 cells overexpressing mPar6 (MDCK-ErbB2-Par6) were also generated by infection and verified by anti;par6 or anti-Flag immunoblots. For morphological and cell cycle studies, all MDCK derived cell lines were platted at a density of 0.5 x 10^6 cells per 0.4μ pore size Transwell inserts (Corning, Corning, NY) and allowed to polarize

for four days. ErbB2 was activated in these polarized monolayers by addition of Dimerizer (1μM) for indicated length of time and the filters were further processed as described below.

Immunofluorescence and microscopy analysis. Filters were fixed in 2% neutral buffered formalin (Sigma), washed three times in PBS: Glycine (130 mM NaCl, 7 mM Na_2HPO_4, 3.5mM NaH_2PO_4, 100 mM Glycine) for 10 minutes. Cells were permeablized for 10 minutes in PBS:0. 2% Triton X-100 at 4^oC, and subsequently rinsed three times in IF buffer (130 mM NaCl, 7 mM Na_2HPO_4, 3.5 mM NaH_2PO_4, 7.7 mM NaN_3. 0.1% Bovine serum albumin, 0.2% Triton X-100, 0.05% Tween 20), for 10 minutes. The filters were cut into small pieces and blocked for 1 hour in blocking buffer (IF buffer plus 10% goat serum). Each piece was stained for different antibody combinations to control for intra-experimental differences. Primary antibodies were typically diluted 1:100 in blocking buffer and incubated for 1.5 – 2.0 hours; filters were washed three times in IF buffer. Alexa fluor conjugated secondary antibodies were diluted 1:100 in blocking buffer and incubated for 50 minutes. Unbound secondary antibodies were washed three times in IF buffer for 20 min. Nuclei were stained with DAPI, and slides were mounted with Prolong antifade (Molecular Probes). Microscopy was preformed using the Apotome software on a Zeiss Axiovert 200M, confocal analysis was preformed with the Zeiss LSM 410 (Carl Zeiss Inc., Thornwood, NY).

A quantitative image analysis method was designed to estimate the disruption of apical basal polarity caused by ErbB2 activation, First, boundaries between the different membrane domains were defined in non-stimulated fully polarized monolayers by addressing the localization of different membrane markers in 0.5 μm non-overlapping X-Z optical sections. The apical domain was defined as a 1.0 μm from the apex of the monolayer and the apical-lateral border was defined as 1.0 – 3.0 μm region from the apex and the remainder (4.0 – 8.0 μm) was defined as the lateral membrane. The presence of this marker outside this standardized boundary was analyzed then in ErbB2 activated filters as an indicator of polarity disruption. For each time point considered, over 200 junctions were analyzed.

Cell cycle analysis. Filters grown as described above were fixed in ice cold 70% ethanol and stained with 20 μg/mL Propidium Iodide (Sigma) in PBS with 1% calf serum and 20 μg/mL RNAseA. Samples were analyzed using an LSRII flow cytometer (Becton Dickinson, San Jose, CA) and 10,000 cells/sample were collected. Data from at least three independent experiments were analyzed using ModFit software (Verity, Topsham, ME).

Par complex immunoprecipitation. MDCK-ErbB2 or 10A.ErbB2 cells were grown to confluency in 10 cm plates. ErbB2 signaling was induced by addition AP1510 (Dimerizer) at concentrations of 500 nm or 1 μm. For immunoprecipitation studies, cells were lysed as described [19]. Anti-mPar3, anti-mPar6, anti-Ha.11, and anti-flag immunoprecipitations and immunoblots were carried out as described earlier [19]

3D morphogenesis assay. 10A.ErbB2 cell lines overexpressing control vector, wtPar6, Par6K19A were generated by retroviral infection as described [6,47]. Each of these cell lines was subsequently infected with a retroviral vector encoding for Bcl-2 and selected to generate 10A.ErbB2.control.Bcl-2, 10A.ErbB2.Par6.Bcl-2 and 10A.ErbB2.Par6K19A.Bcl-2 cell lines. Stable populations were assayed for expression of recombinant proteins and ErbB2-Par6/aPKC interaction (see above) and used for acinar morphogenesis assays as described [6,47]. Day 4 acinar structures were stimulated with 1 μm AP1510 or left untreated for 4 days. At day 8, morphology was assessed by phase microscopy and cells were fixed and processed for immunoflourescence analysis as described elsewhere [6,47]. Structure size was measured using Axiovision 4.4 software (Zeiss) and the number of multistructures was counted. At least 400 structures from 3 different experiments were studied for each experimental condition, except for the Bcl-2 cell lines for which at least 200 cells from 2 independent experiments were counted, and size data were subjected to statistical analysis (see below).

Statistical Analysis: The surface data was log-transformed to achieve normal distribution, checked by the Shapiro-Francia test. We then performed ANOVA analysis on the transformed data, assessing differences by orthogonal and interaction contrasts between the control and treated groups. Differences were considered significant if the p value was less than 0.05 or the Bonferroni adjusted 0.05 value. All statistical procedures were carried out on SPSS 11.0 (SPSS Inc. Chicago IL).

CELL LINE	BASAL (control)	STIMULATION (-/+ ErbB2)	INTERACTION (Par6K19A)
10A.ErbB2.vector	X	P<0.0005	P<0.0005
10A.ErbB2.Par6	P=0.509	P<0.0005	P<0.0005
10A.ErbB2.Par6K19A	P=0.509	P<0.0005	X

Table 1: Summary of two-way ANOVA statistical analysis of acinar size (see Material and Methods). BASAL represents the comparison between unstimulated acini from control cells and cells overexpressing different Par6 versions by orthogonal contrast. STIMULATION refers to the comparison within each cell line between stimulated and non-stimulated conditions by non-orthogonal contrasts. INTERACTION represents the comparison of the size of the effect of ErbB2 stimulation between cells overexpressing Par6K19A and control and Par6 overexpressing cells by interaction contrasts.

Acknowledgements:

We would like to thank members of the Muthuswamy laboratory for all their input and helpful discussions. ARIAD pharmaceutical for synthetic dimerizing ligand, AP1510. SKM was supported by CA098830, The V foundation Scholar award, Rita Allen Scholar award, FACT, Glencove cares and LIBC foundation. TH was supported by DAMD17-03-1-0194. MEN was supported by DAMD17-03-0193.

References:

1. Schnitt, S. J. & Connolly, J. L. in *Diseases of the Breast* (eds. Harris, J., Lippman, M. E., Morrow, M. & Osborne, K.) 77 - 99 (Lippincott Williams & Wilkins, Philadelphia, 2004).
2. Polosukhin, V. V. Ultrastructural of the bronchial epithelium in chronic inflammation. *Ultrastruct Pathol* **25**, 119-28 (2001).
3. Dranoff, G. Cytokines in cancer pathogenesis and cancer therapy. *Nat Rev Cancer* **4**, 11-22 (2004).
4. Drubin, D. G. & Nelson, W. J. Origins of cell polarity. *Cell* **84**, 335-44 (1996).
5. Schneeberger, E. E. & Lynch, R. D. The tight junction: a multifunctional complex. *Am J Physiol Cell Physiol* **286**, C1213-28 (2004).
6. Muthuswamy, S. K., Li, D., Lelievre, S., Bissell, M. J. & Brugge, J. S. ErbB2, but not ErbB1, reinitiates proliferation and induces luminal repopulation in epithelial acini. *Nat Cell Biol* **3**, 785-92 (2001).
7. Schoenenberger, C. A., Zuk, A., Kendall, D. & Matlin, K. S. Multilayering and loss of apical polarity in MDCK cells transformed with viral K-ras. *J Cell Biol* **112**, 873-89 (1991).
8. Li, D. & Mrsny, R. J. Oncogenic Raf-1 disrupts epithelial tight junctions via downregulation of occludin. *J Cell Biol* **148**, 791-800 (2000).
9. Reichmann, E. et al. Activation of an inducible c-FosER fusion protein causes loss of epithelial polarity and triggers epithelial-fibroblastoid cell conversion. *Cell* **71**, 1103-16 (1992).
10. Fialka, I. et al. The estrogen-dependent c-JunER protein causes a reversible loss of mammary epithelial cell polarity involving a destabilization of adherens junctions. *J Cell Biol* **132**, 1115-32 (1996).
11. Jou, T. S., Schneeberger, E. E. & Nelson, W. J. Structural and functional regulation of tight junctions by RhoA and Rac1 small GTPases. *J Cell Biol* **142**, 101-15 (1998).
12. Rojas, R., Ruiz, W. G., Leung, S. M., Jou, T. S. & Apodaca, G. Cdc42-dependent modulation of tight junctions and membrane protein traffic in polarized Madin-Darby canine kidney cells. *Mol Biol Cell* **12**, 2257-74 (2001).
13. Behrens, J. et al. Loss of epithelial differentiation and gain of invasiveness correlates with tyrosine phosphorylation of the E-cadherin/beta-catenin complex in cells transformed with a temperature-sensitive v-SRC gene. *J Cell Biol* **120**, 757-66 (1993).
14. Bilder, D. Epithelial polarity and proliferation control: links from the Drosophila neoplastic tumor suppressors. *Genes Dev* **18**, 1909-25 (2004).
15. Nelson, W. J. Adaptation of core mechanisms to generate cell polarity. *Nature* **422**, 766-74 (2003).
16. Stoll, M. et al. Genetic variation in DLG5 is associated with inflammatory bowel disease. *Nat Genet* **36**, 476-80 (2004).
17. Ragaz, J. in *Diseases of the Breast* (eds. Harris, J., Lippman, M. E., Morrow, M. & Osborne, K.) 619 - 652 (Lippincott Williams & Wilkins, Philadelphia, 2004).
18. Hynes, N. E. & Lane, H. A. ERBB receptors and cancer: the complexity of targeted inhibitors. *Nat Rev Cancer* **5**, 341-54 (2005).
19. Muthuswamy, S. K., Gilman, M. & Brugge, J. S. Controlled dimerization of ErbB receptors provides evidence for differential signaling by homo- and heterodimers. *Mol Cell Biol* **19**, 6845-57 (1999).
20. Rodriguez-Boulan, E., Kreitzer, G. & Musch, A. Organization of vesicular trafficking in epithelia. *Nat Rev Mol Cell Biol* **6**, 233-47 (2005).
21. Amara, J. F. et al. A versatile synthetic dimerizer for the regulation of protein-protein interactions. *Proc Natl Acad Sci U S A* **94**, 10618-23. (1997).

22. Etienne-Manneville, S. & Hall, A. Cell polarity: Par6, aPKC and cytoskeletal crosstalk. *Curr Opin Cell Biol* **15**, 67-72 (2003).
23. Macara, I. G. Par proteins: partners in polarization. *Curr Biol* **14**, R160-2 (2004).
24. Margolis, B. & Borg, J. P. Apicobasal polarity complexes. *J Cell Sci* **118**, 5157-9 (2005).
25. Suzuki, A. & Ohno, S. The PAR-aPKC system: lessons in polarity. *J Cell Sci* **119**, 979-87 (2006).
26. Yamanaka, T. et al. PAR-6 regulates aPKC activity in a novel way and mediates cell-cell contact-induced formation of the epithelial junctional complex. *Genes Cells* **6**, 721-31 (2001).
27. Ozdamar, B. et al. Regulation of the polarity protein Par6 by TGFbeta receptors controls epithelial cell plasticity. *Science* **307**, 1603-9 (2005).
28. Suzuki, A. et al. Atypical protein kinase C is involved in the evolutionarily conserved par protein complex and plays a critical role in establishing epithelia-specific junctional structures. *J Cell Biol* **152**, 1183-96 (2001).
29. Noda, Y. et al. Molecular recognition in dimerization between PB1 domains. *J Biol Chem* **278**, 43516-24 (2003).
30. Wilson, M. I., Gill, D. J., Perisic, O., Quinn, M. T. & Williams, R. L. PB1 domain-mediated heterodimerization in NADPH oxidase and signaling complexes of atypical protein kinase C with Par6 and p62. *Mol Cell* **12**, 39-50 (2003).
31. Loden, M., Perris, F., Nielsen, N. H., Emdin, S. O. & Landberg, G. C-erbB2, p27 and G1/S aberrations in human primary breast cancer. *Anticancer Res* **23**, 2053-61 (2003).
32. Debnath, J. et al. The role of apoptosis in creating and maintaining luminal space within normal and oncogene-expressing mammary acini. *Cell* **111**, 29-40 (2002).
33. Liu, H., Radisky, D. C., Wang, F. & Bissell, M. J. Polarity and proliferation are controlled by distinct signaling pathways downstream of PI3-kinase in breast epithelial tumor cells. *J Cell Biol* **164**, 603-12 (2004).
34. Guo, W. et al. beta4 Integrin Amplifies ErbB2 Signaling to Promote Mammary Tumorigenesis. *Cell* **126**, 489-502 (2006).
35. Downward, J. Targeting RAS signalling pathways in cancer therapy. *Nat Rev Cancer* **3**, 11-22 (2003).
36. Yu, H. & Jove, R. The STATs of cancer--new molecular targets come of age. *Nat Rev Cancer* **4**, 97-105 (2004).
37. Citri, A. & Yarden, Y. EGF-ERBB signalling: towards the systems level. *Nat Rev Mol Cell Biol* **7**, 505-16 (2006).
38. Howley, P. M., Munger, K., Werness, B. A., Phelps, W. C. & Schlegel, R. Molecular mechanisms of transformation by the human papillomaviruses. *Princess Takamatsu Symp* **20**, 199-206 (1989).
39. Munger, K., Scheffner, M., Huibregtse, J. M. & Howley, P. M. Interactions of HPV E6 and E7 oncoproteins with tumour suppressor gene products. *Cancer Surv* **12**, 197-217 (1992).
40. Nakagawa, S. & Huibregtse, J. M. Human scribble (Vartul) is targeted for ubiquitin-mediated degradation by the high-risk papillomavirus E6 proteins and the E6AP ubiquitin-protein ligase. *Mol Cell Biol* **20**, 8244-53 (2000).
41. Kiyono, T. et al. Binding of high-risk human papillomavirus E6 oncoproteins to the human homologue of the Drosophila discs large tumor suppressor protein. *Proc Natl Acad Sci U S A* **94**, 11612-6 (1997).
42. Muthuswamy, S. K. ErbB2 Makes beta4 Integrin an Accomplice in Tumorigenesis. *Cell* **126**, 443-5 (2006).
43. Regala, R. P. et al. Atypical protein kinase C iota is an oncogene in human non-small cell lung cancer. *Cancer Res* **65**, 8905-11 (2005).

44. Eder, A. M. et al. Atypical PKCiota contributes to poor prognosis through loss of apical-basal polarity and cyclin E overexpression in ovarian cancer. *Proc Natl Acad Sci U S A* **102**, 12519-24 (2005).
45. Stallings-Mann, M. et al. A novel small-molecule inhibitor of protein kinase Ciota blocks transformed growth of non-small-cell lung cancer cells. *Cancer Res* **66**, 1767-74 (2006).
46. Lin, D. et al. A mammalian PAR-3-PAR-6 complex implicated in Cdc42/Rac1 and aPKC signalling and cell polarity. *Nat Cell Biol* **2**, 540-7 (2000).
47. Debnath, J., Muthuswamy, S. K. & Brugge, J. S. Morphogenesis and oncogenesis of MCF-10A mammary epithelial acini grown in three-dimensional basement membrane cultures. *Methods* **30**, 256-68 (2003).

Figure legends:

Figure 1. ErbB2 initiates disruption of apical-basal polarity at the apical-basal border.

A: Immunofluorescence study of polarity markers in MDCK-ErbB2. Cells were fixed at the stated time points and stained for polarized membrane markers: ZO-1 (tight junctions), gp135 (apical membrane); and nuclei were costained with DAPI. The top and side boxes represent X-Z axis while the boxed area represent X-Y axis. Red arrow marks the point of plane in X-Z axis that was chosen for the X-Y image. Scale bar: 100μm. B: Time course analysis of ErbB2-induced loss of apical-basal polarity. MDCK-ErbB2 cells stimulated for the stated time points were processed as described above. Cartoon shows optical sections at 0.5μm intervals along the X-Z axis that were analyzed for presence of absence of apical proteins, gp135 and ZO-1. Lines mark 2μm sections along the X-Z axis. Arrow marks the 4μm sections depicted. C: Approximately 2000 junctions were analyzed to determine that ZO-1 was restricted to 2.0μm from the apex (0 hrs). The presence of ZO-1 below the 2.0μm sections was quantitated (B, green graph) for at least 200 junctions and values represent mean ± standard deviation of three independent experiments. The area with multilayered regions was measured using Zeiss axiovision software as described in the methods section. The graph (B, Red) represents the mean ± standard deviation of three independent experiments. D: Changes in proliferation status were monitored by Flow Cytometry and mean ± standard deviation of at least three independent experiments are shown.

Figure 2. ErbB2 disrupts the Par complex and recruits Par6/aPKC.

A: MDCK-ErbB2 cells overexpressing flag-tagged Par6 (MDCK-ErbB2-Par6) were treated with dimerizer for ErbB2 activation and immunostained for flag-tagged Par6; nuclei were costained with DAPI. Extracts from these cells with unactivated (0) or activated (15 – 120 minutes) ErbB2 were used for immunoprecipitation with anti-Par6 antisera (D) or anti-Par3 (E) and immunoblotted with anti-HA or anti-aPKC antisera. Extracts from MDCK-ErbB2 cells with unactivated (0) or activated (30 – 120 minutes) ErbB2 were used for immunoprecipitation with anti-Par6 antisera (B) or anti-Par3 (C) and immunoblotted with anti-aPKC antisera.

Figure 3. Par6/aPKC is required for ErbB2-induced transformation of MCF10A 3D acini.

A: Extracts from 10A.ErbB2 cells overexpressing Par6 or Par6K19A were used for immunoprecipitation with anti-Par6 antisera and immunoblotted with anti-HA or anti-aPKC antisera. B: Phase images of unstimulated day 8 acinar structures (left panels) or day 8

structures in which ErbB2 was activated on day 4 (right panels). Inserts show details of acinar morphology. C: The number of multistructures was quantified by image analysis. Data are means ±SD from three different experiments. D: Distribution of acini size under different conditions plotted as a box plot. The box outlines 50% of the data with median value drawn as a white line and the dark lines represent acini of different sizes. The data represents more than 4000 individual structures compiled from three independent experiments. Scale bar: 100μm.

Figure 4. ErbB2-Par6/aPKC interaction is not required for ErbB2-induced proliferation.
A: Ki67 staining of day 8 acinar structures from 10A.B2.vector (vector) or 10A.B2.Par6 (Par6), or 10A.B2.Par6K19A (Par6K19A) cells grown with (right panels) or without receptor activation (left panels). B: Flow cytometry analysis of the proliferation increase induced by ErbB2 in normal plastic culture condition in these cell lines. Data are means of S/G2 phase percentage ±SD from 3 independent experiments.

Figure 5. Increased apoptosis in response to ErbB2 activation in cells expressing Par6K19A.
A: Day 8 acinar structures from 10A.B2.vector (vector) or 10A.B2.Par6.Bcl2 (Par6 Bcl2), or 10A.B2.Par6K19A.Bcl2 (Par6K19A Bcl2) cells grown with (right panels) or without receptor activation (left panels) were immunostained with the apoptotic marker cleaved caspase 3. Nuclei were stained with DAPI. B: Day 16 acinar structures from 10A.B2.Par6 (Par6) or 10A.B2.Par6K19A (Par6K19A) grown with (right panels) or without receptor activation (left panels). Nuclei were stained with DAPI to study acinar organization and lumen formation. Scale bar: 50μm.

Figure 6. Bcl-2 expression partially rescues ErbB2-induced disruption of epithelial organization.
A: Overexpression of Bcl-2 was assessed by immunoblot, extracts from 10A.B2.Par6, 10A.B2.Par6.Bcl.2, 10A.B2.Par6K19A and 10A.B2.Par6k19A.Bcl-2 were blotted with anti-Bcl-2 antisera and anti-actin antisera. B: Phase images of day 8 acinar structures unstimulated (top panels) or stimulated (bottom panels) for 4 days for ErbB2 activation from 10A.B2.Par6K19A, 10A.B2.Par6.Bcl-2 or 10A.B2.Par6K19A.Bcl-2 cells. C: Acinar structures were immunostained for cleaved caspase 3, nuclei were stained with DAPI. Inserts show details of acinar morphology and staining. Scale bar: 50μm. D: Number of multistructures from the stated cell lines with or

without ErbB2 activation was quantified by image analysis. Data are represented as means ± SD from at least 400 structures from 2 independent experiments.

Suppl. Figure 1. ErbB2 activation disrupts polarized organization of epithelial cells.

A: Immunoblot analysis of ErbB2 expression and activation of ErbB2. MDCK.ErbB2 cells were stimulated with dimerizer for the indicated times and lysates were blotted with anti-phosphotyrosine antisera and anti-HA antisera. B: MDCK.ErbB2 cells with (left panels) or without ErbB2 activation were fixed and stained for different polarized membrane markers: ZO-1 and E-cadherin (top panels) or ZO-1 and GM130 (bottom panels). Nuclei were stained with DAPI. Red arrows mark the plane of the X-Z section depicted on the X-Y section.

Suppl. Figure 2. Reversion of ErbB2-induced disruption of apical polarity and changes in tight junction permeability.

A: ErbB2 was activated in polarized MDCK-ErbB2 cells for 24 hours (top panels) and dimerizer was washed away and monolayers incubated for another 48 hours (bottom panels). Cells were stained for apical marker gp135 and tight junction marker ZO-1, nuclei were stained with DAPI. X-Y optical sections representing apical-lateral border and lateral membrane are shown. B: For functional polarity analysis, MDCK-ErbB2 were allowed to polarize and ErbB2 was activated for 24 hours. Control (unstim) or ErbB2 activated (stim), monolayers were incubated for 4 hours with Dextran 10,000 MW (Molecular Probes) on the upper chamber, and fluorescent Dextran in the bottom chamber was measured by fluorimetry.

Suppl. Figure 3. Time course analysis of ErbB2-induced disruption of apical-basal polarity.

A: MDCK.ErbB2 cells were stimulated for the indicated times and fixed and stained as described. Optical sections at 0.5μm intervals along the X-Z axis were analyzed for presence of absence of the apical protein gp135, and ZO-1. X-Y sections at different distances from the apical surface were analyzed for the presence of gp135 and/or ZO-1. ZO-1 mislocalization was more prominent at tricellular junctions (white arrows). Red arrows mark the plane of the X-Z section depicted on the X-Y section.

Figure-1 (Muthuswamy)

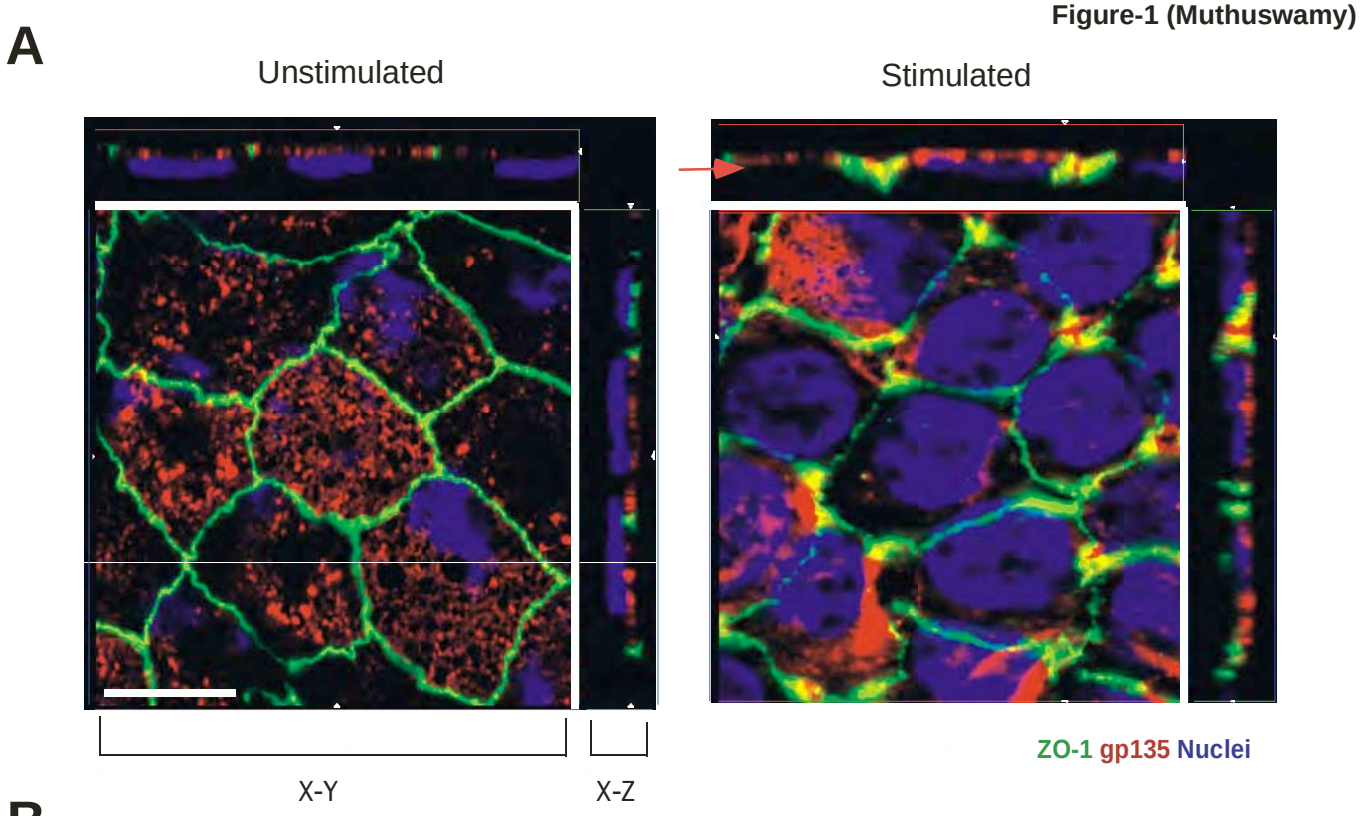

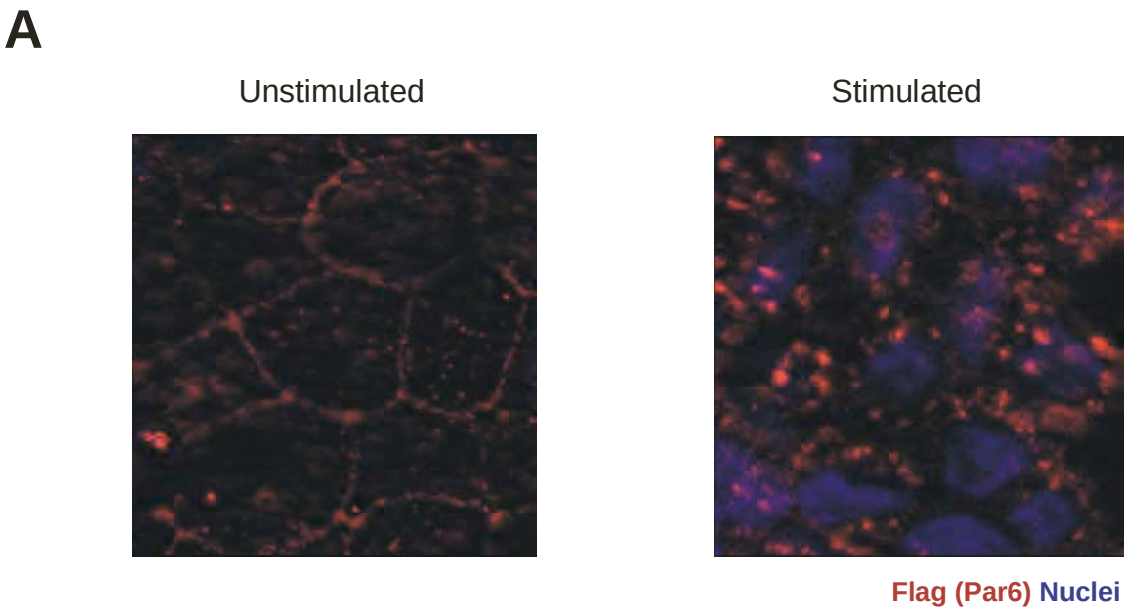
A
Unstimulated
Stimulated
Flag (Par6) Nuclei
B
IP: Par6
0
30
60
120
81
IB: aPKC
43
IB: Par6
C
IP:Par3
0
30
60
120
81
IB: aPKC
180
IB: Par3
D
IP: Par6
0
15
30
60
120
181.8
IB: HA (ErbB2)
82.2
IB: aPKC
48.8
IB: Flag (Par6)
E
IP:Par3
0
15
30
60
120
181.8
IB: HA (ErbB2)
181.8
IB: Par3

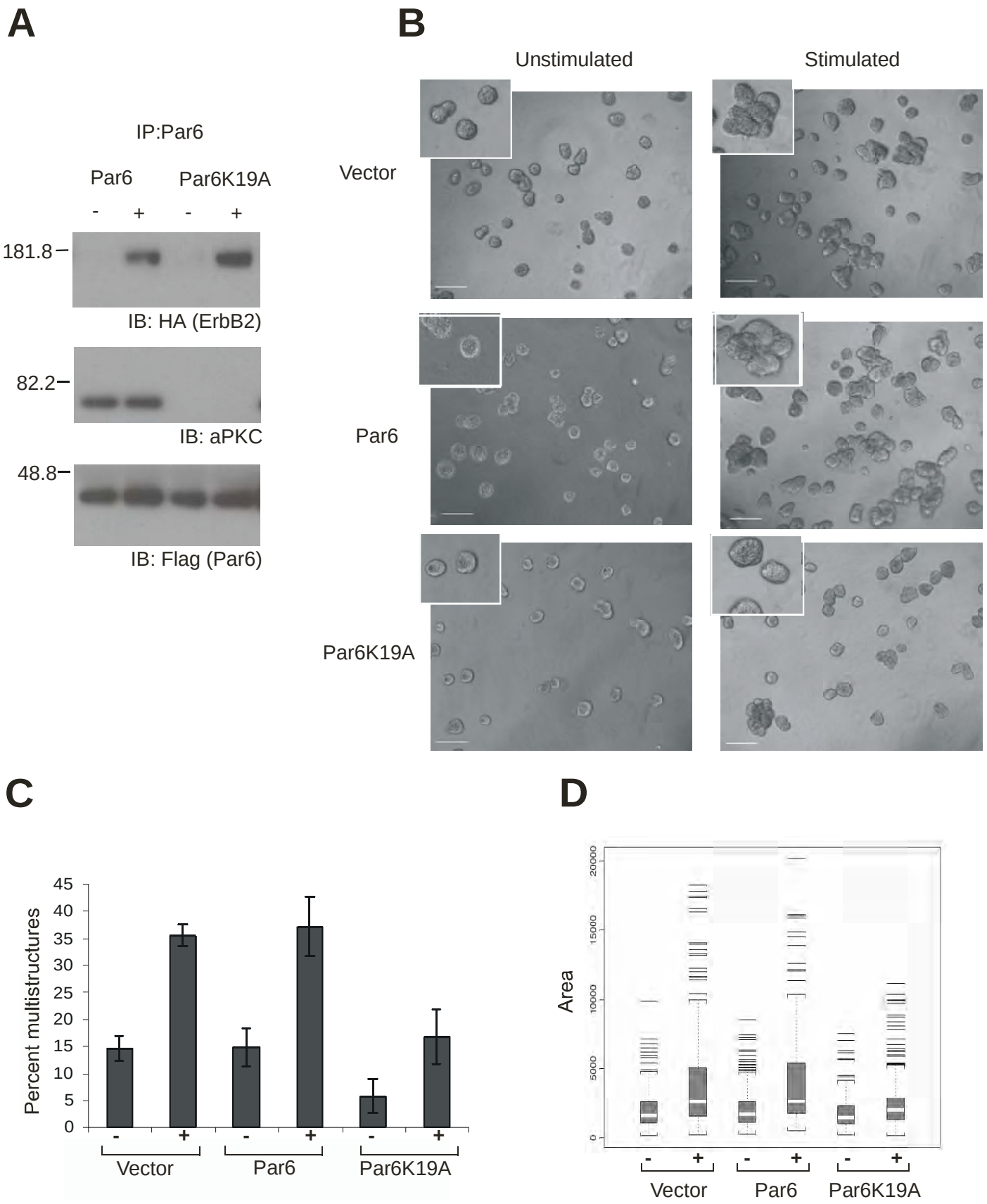
A
IP:Par6
Par6
Par6K19A
- + - +
181.8
IB: HA (ErbB2)
82.2
IB: aPKC
48.8
IB: Flag (Par6)
B
Unstimulated
Stimulated
Vector
Par6
Par6K19A
C
Percent multistructures
45
40
35
30
25
20
15
10
5
0
- + - + - +
Vector
Par6
Par6K19A
D
Area
20000
15000
10000
5000
0
- + - + - +
Vector
Par6
Par6K19A

Figure-4 (Muthuswamy)

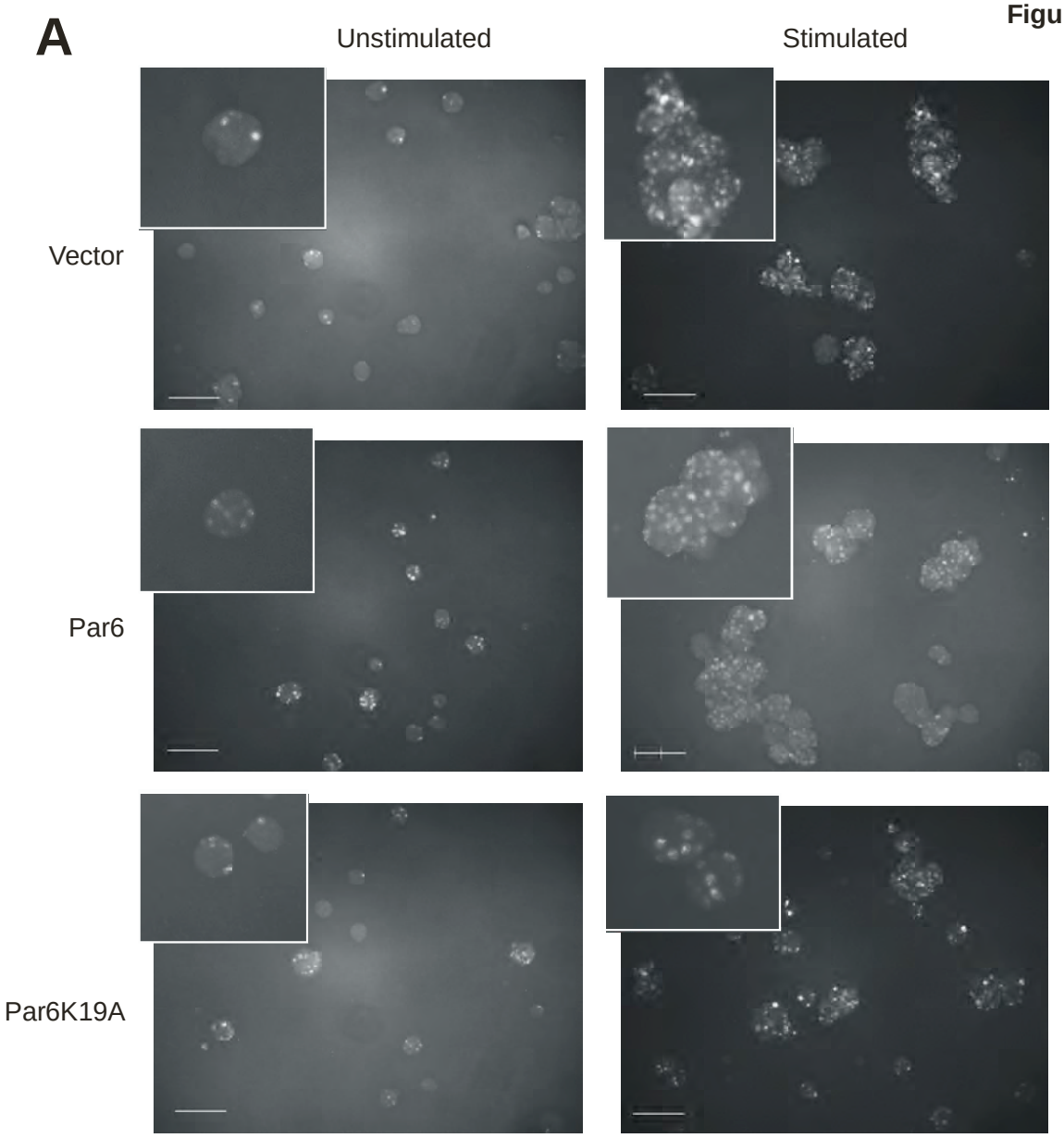

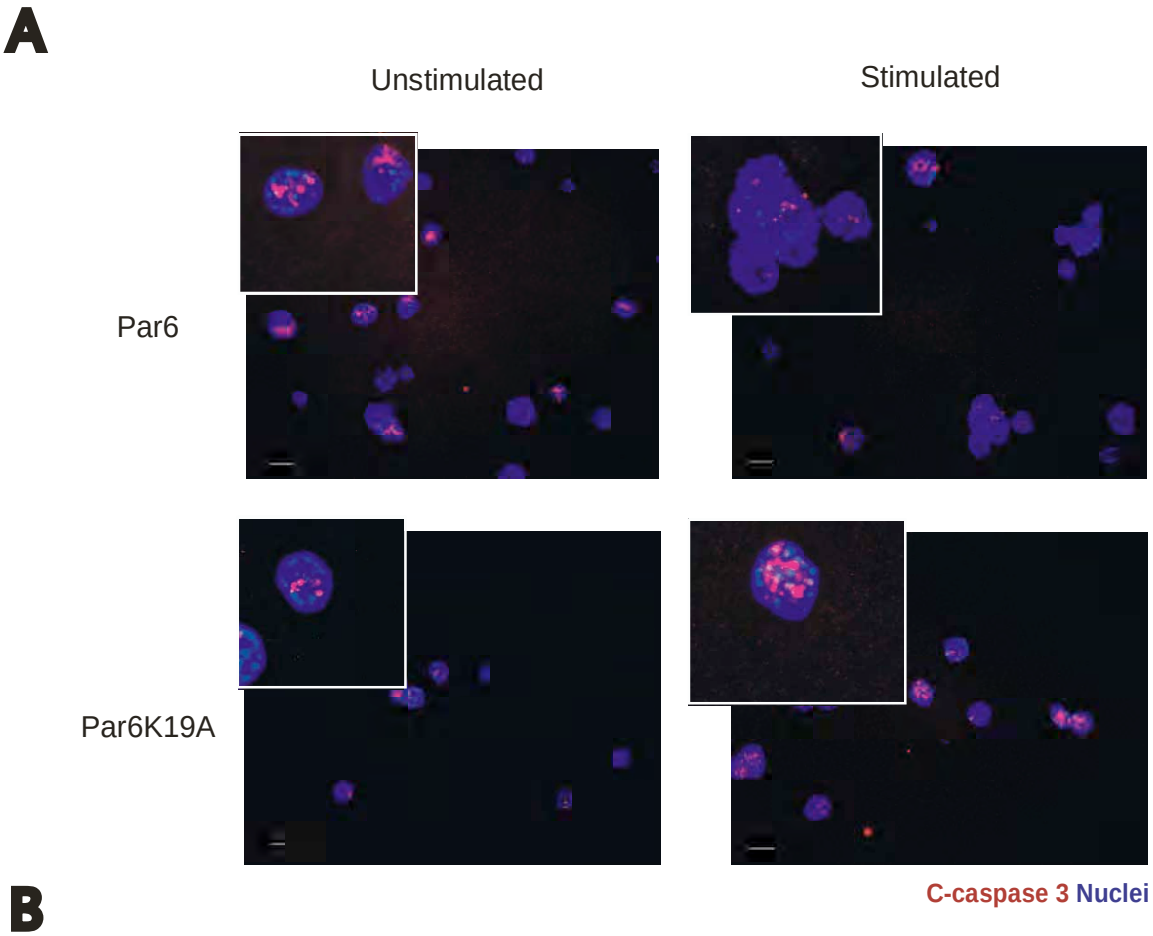
A
Unstimulated
Stimulated
Par6
Par6K19A
B
C-caspase 3 Nuclei
Par6
Par6K19A

Figure-6 (Muthuswamy)

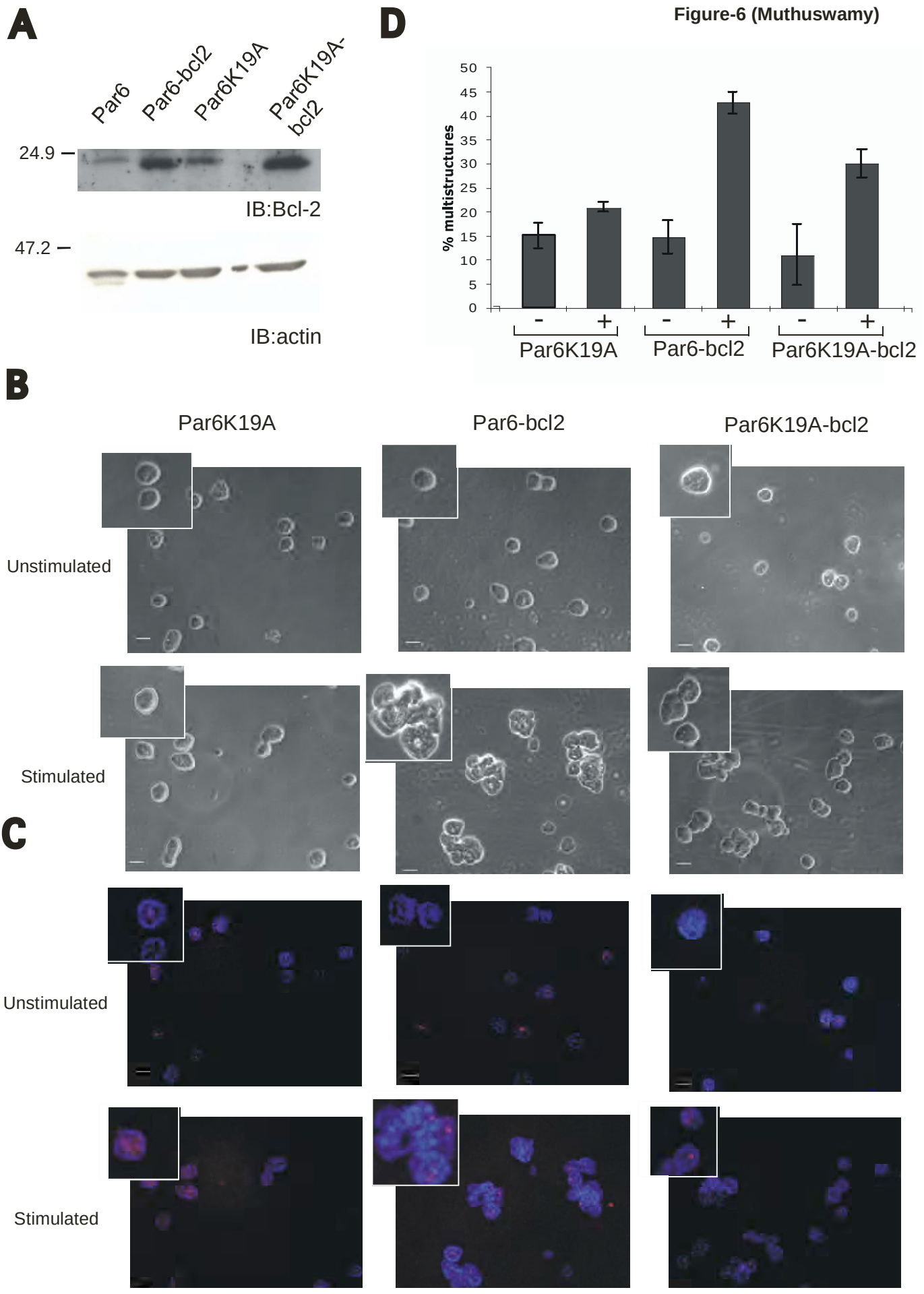

CELL LINE	BASAL (control)	STIMULATION (-/+ ErbB2)	INTERACTION (Par6K19A)
10A.ErbB2.vector	X	P<0.0005	P<0.0005
10A.ErbB2.Par6	P=0.509	P<0.0005	P<0.0005
10A.ErbB2.Par6K19A	P=0.509	P<0.0005	X

Table 1: Summary of two-way ANOVA statistical analysis of acinar size (see Material and Methods). BASAL represents the comparison between unstimulated acini from control cells and cells overexpressing different Par6 versions by orthogonal contrast. STIMULATION refers to the comparison within each cell line between stimulated and non-stimulated conditions by non-orthogonal contrasts. INTERACTION represents the comparison of the size of the effect of ErbB2 stimulation between cells overexpressing Par6K19A and control and Par6 overexpressing cells by interaction contrasts.